iScience

CellPress

Article

Chromatin Remodeling BAF155 Subunit Regulates the Genesis of Basal Progenitors in Developing Cortex

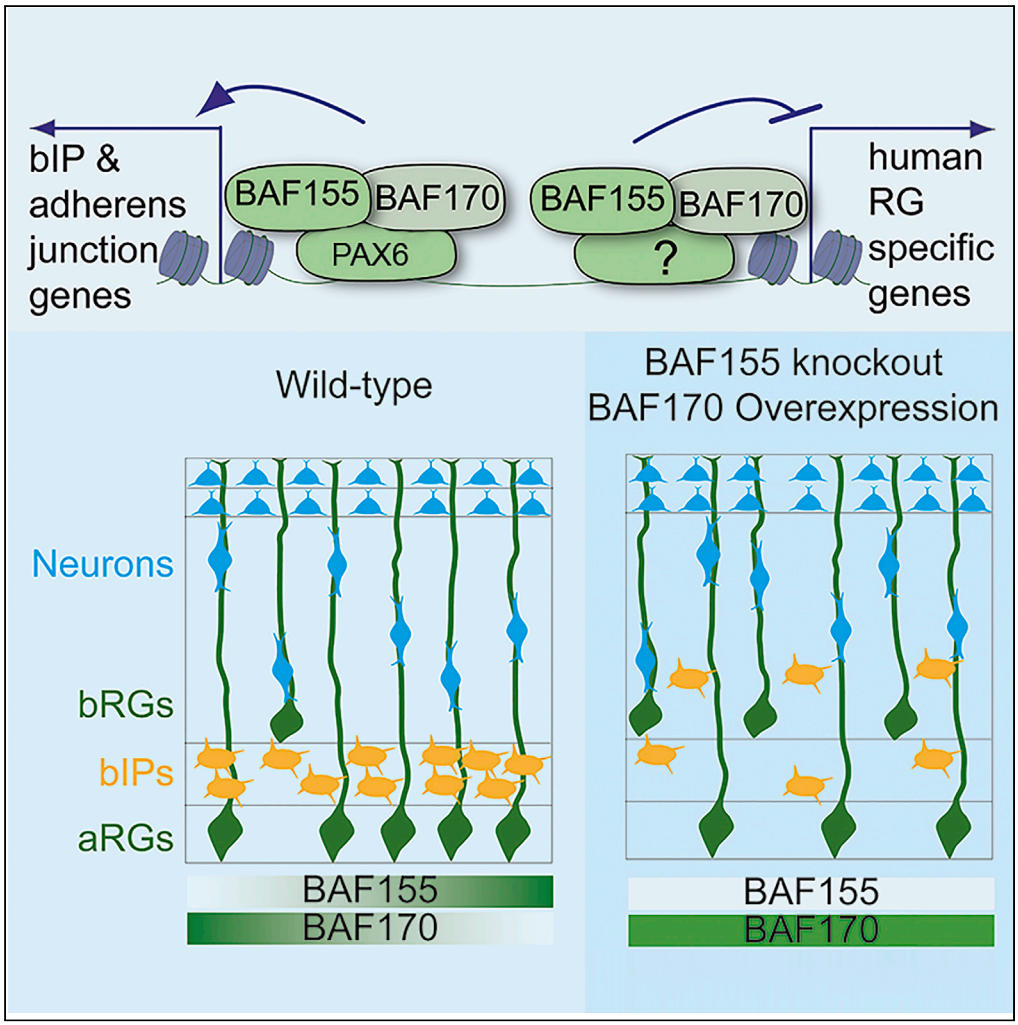

Ramanathan Narayanan, Linh Pham, Cemil Kerimoglu, ..., Anastassia Stoykova, Jochen F. Staiger, Tran Tuoc

astoyko@gwdg.de (A.S.)
tran.tuoc@med.uni-goettingen.de (T.T.)

HIGHLIGHTS

BAF155 potentiates PAX6 transcriptional activity

BAF155 and PAX6 co-regulate bIP genesis in developing cerebral cortex

BAF155 and PAX6 control bRG genesis through aRG delamination non-cell-autonomously

BAF155 suppresses the expression of human RG-specific genes in developing mouse cortex

DATA AND SOFTWARE AVAILABILITY

GSE106711

Narayanan et al., iScience 4, 109–126
June 29, 2018
https://doi.org/10.1016/j.isci.2018.05.014

iScience

CellPress

Article

Chromatin Remodeling BAF155 Subunit Regulates the Genesis of Basal Progenitors in Developing Cortex

Ramanathan Narayanan,[1,7] Linh Pham,[1] Cemil Kerimoglu,[2] Takashi Watanabe,[3] Ricardo Castro Hernandez,[1] Godwin Sokpor,[1] Pauline Antonie Ulmke,[1] Kamila A. Kiszka,[1,5] Anton B. Tonchev,[3,6] Joachim Rosenbusch,[1] Rho H. Seong,[4] Ulrike Teichmann,[3] Jens Frahm,[3] Andre Fischer,[2,5] Stefan Bonn,[2] Anastassia Stoykova,[3,5,*] Jochen F. Staiger,[1,5] and Tran Tuoc[1,5,8,*]

SUMMARY

The abundance of basal progenitors (BPs), basal radial glia progenitors (bRGs) and basal intermediate progenitors (bIPs), in primate brain has been correlated to the high degree of cortical folding. Here we examined the role of BAF155, a subunit of the chromatin remodeling BAF complex, in generation of cortical progenitor heterogeneity. The conditional deletion of BAF155 led to diminished bIP pool and increased number of bRGs, due to delamination of apical RGs. We found that BAF155 is required for normal activity of neurogenic transcription factor PAX6, thus controlling the expression of genes that are involved in bIP specification, cell-cell interaction, and establishment of adherens junction. In a PAX6-dependent manner, BAF155 regulates the expression of the CDC42 effector protein CEP4, thereby controlling progenitor delamination. Furthermore, BAF155-dependent chromatin remodeling seems to exert a specific role in the genesis of BPs through the regulation of human RG-specific genes (such as *Foxn4*) that possibly acquired evolutionary significance.

INTRODUCTION

The mammalian cerebral cortex is a sheet of cells covering the cerebrum and responsible for complex brain functions, such as sensory perception, motor response, and cognition, especially in higher primates. Cortical development is a tightly regulated process that involves waves of differentiative divisions of multiple progenitor types in the forebrain germinative zones, the ventricular (VZ) and subventricular zone (SVZ), to generate specific neuronal subtypes that make up the six cortical layers (Borrell and Gotz, 2014; Gotz and Huttner, 2005; Kriegstein et al., 2006; Leone et al., 2008; Molyneaux et al., 2007; O'Leary et al., 2007; Tuoc et al., 2014). Based on morphology, lineage commitment, molecular characteristics, and the site of cell division, the progenitor cells of the developing cortex are grouped into two major categories: apical (APs) and basal progenitors (BPs). The APs are cells that divide at the apical surface of the VZ and include neuroepithelial cells (NEs) and apical radial glial cells (aRGs). The BPs are derivatives of APs that divide in the SVZ and include two subtypes, the basal radial glial cells (bRGs) and basal intermediate progenitors (bIPs) (Lui et al., 2011; Florio and Huttner, 2014; Taverna et al., 2014; Tuoc et al., 2014; Dehay et al., 2015; Fernandez et al., 2016). In the course of mammalian evolution, the cerebral cortex has diversified from a smooth (lissencephalic) cortex in rodents to a folded (gyrencephalic) cortex in primates, including human. A specific trait of the primate and human cortices is the abundant presence of bRGs and bIPs, which together form a distinct zone, the outer sub-ventricular zone (oSVZ), located basal to the inner SVZ (iSVZ; identical to SVZ in rodents) (Betizeau et al., 2013; Fietz et al., 2010; Hansen et al., 2010; Kelava et al., 2012; Lukaszewicz et al., 2005; Wang et al., 2011). The remarkable enlargement of the oSVZ during evolution is strongly associated with an increased neuronal output, cortical expansion, and folding of the primate/human cortex (Borrell and Gotz, 2014; Dehay et al., 2015; Fernandez et al., 2016; Florio and Huttner, 2014; Lui et al., 2011; Sun and Hevner, 2014; Taverna et al., 2014; Tuoc et al., 2014). Despite the importance of the molecular machinery that regulates the genesis of BPs in cerebral cortex evolution, it is only beginning to be elucidated.

The transcription factor (TF) PAX6 is involved in many processes of mammalian corticogenesis, including generation of bRGs (Asami et al., 2011; Wong et al., 2015) and bIP specification (Georgala et al., 2011; Gotz et al., 1998; Quinn et al., 2006; Sansom et al., 2009; Tuoc et al., 2009). Recently, we and other groups reported that TF PAX6 interacts with multiple subunits of the chromatin-remodeling mSWI/SNF

[1]Institute of Neuroanatomy, University Medical Center, Georg-August-University, 37075 Goettingen, Germany

[2]German Center for Neurodegenerative Diseases, 37075 Goettingen, Germany

[3]Max-Planck-Institute for Biophysical Chemistry, 37077 Goettingen, Germany

[4]Department of Biological Sciences, Institute of Molecular Biology and Genetics, Seoul National University, Seoul 08826, Korea

[5]DFG, Center for Molecular Physiology of the Brain (CMPB), 37075 Goettingen, Germany

[6]Department of Anatomy and Cell Biology, Medical University-Varna, BG-9002 Varna, Bulgaria

[7]Present address: Lab of Systems Neuroscience, Institute for Neuroscience, Department of Health Science and Technology, Swiss Federal Institute of Technology (ETH), 8057 Zurich, Switzerland

[8]Lead Contact

*Correspondence: astoyko@gwdg.de (A.S.), tran.tuoc@med.uni-goettingen.de (T.T.)

https://doi.org/10.1016/j.isci.2018.05.014

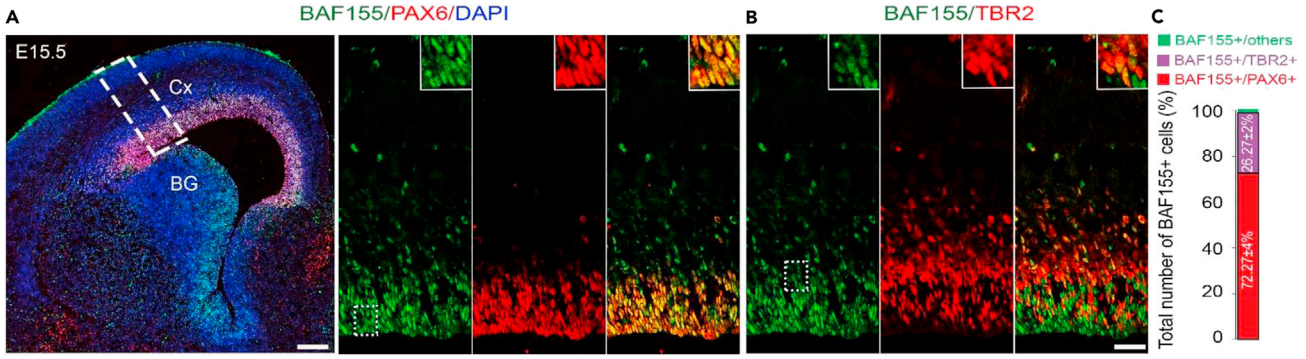

Figure 1. Expression of BAF155 in Developing Cerebral Cortex

(A and B) Confocal imaging of coronal wild-type brain sections at E15.5 after immunostaining for BAF155 and RG marker PAX6 (A) or BAF155 and bIP marker TBR2 (B). Higher magnification of the VZ (white box) is presented in the inner panel.

(C) Statistical analysis revealed that most of BAF155+ cells are PAX6+ aRGs (72 ± 4%), whereas BAF155+/TBR2+ bIPs (26 ± 1.89%) were less than one-third of the BAF155+ cells. Abbreviations: VZ, ventricular zone; RG, radial glia; bIP, basal intermediate progenitor. Scale bars, 100 μm (A), 25 μm (B). See also Figure S1.

(or BRG1/BRM-associated factor, BAF) complex (Bachmann et al., 2016; Ninkovic et al., 2013; Tuoc et al., 2013a, 2013b). More specifically, we found that temporal interaction between TF PAX6 and BAF170 during early corticogenesis (in mouse, E10.5-E14.5) leads to down-regulation of bIP-specific gene expression by recruiting a transcriptional co-repressor complex to PAX6 downstream target genes, thus prohibiting bIP genesis (Tuoc et al., 2013a). In contrast, in the absence of BAF170, as seen in E14.5-E16.5 developing mouse cortex, the BAF complex includes an additional BAF155 subunit, which causes augmentation of the pool of bIPs with formation of a thicker cortex.

In this study, we examined the role of BAF155 in cortical development. We found that, BAF155 potentiates PAX6-dependent transcriptional activity in the developing mouse cortex such that the synergistic interaction between BAF155 and PAX6 controls the fate choice of aRG, hence promoting bIP genesis but suppressing the genesis of bRGs. We show results suggesting a cell-autonomous role for BAF155 in regulating aRG division and non-cell-autonomous mechanisms (PAX6-dependent and PAX6-independent) that appear to underlie the delamination of aRGs from the VZ to generate bRGs.

RESULTS

Expression of BAF155 in Cortical Progenitors and Conditional Inactivation of *Baf155* in Developing Mouse Cortex

Our previous study revealed a dynamic competition between BAF170 and BAF155 subunits within the BAF complex during progression of cortical neurogenesis and that they display complementary expression patterns (Tuoc et al., 2013a). Following a high expression during early corticogenesis (E10.5-E13.5), the expression of BAF170 in progenitors progressively decreases, becoming nearly absent during E15.5. In contrast, following a low expression during earlier stages, the expression of BAF155 peaks at E15.5-E16.5 (Tuoc et al., 2013a). To define which of the progenitor populations (in VZ or SVZ) expresses BAF155, we performed dual-IHC on cortical sections from E15.5 wild-type (WT) embryos with antibodies for BAF155 and markers for cortical progenitor subtype, including PAX6 for RG (Gotz et al., 1998) and TBR2 for bIPs (Hevner et al., 2006), followed by quantification of the double-positive cell populations: BAF155+PAX6+ and BAF155+TBR2+. We found around 72 ± 4% of BAF155+ cells to be PAX6+, whereas only 26 ± 1.89% were TBR2+ cells, implying that BAF155 co-localized predominantly with the RG marker PAX6 in the VZ (Figure 1A) as compared with the bIP marker TBR2 in the SVZ (Figure 1B).

To investigate the functions of BAF155 *in vivo*, we generated cortex-specific *Baf155* knockout mice by crossing floxed *Baf155* (*Baf155*$^{fl/fl}$) mice (Choi et al., 2012) with the *Emx1-Cre* line, in which Cre-recombinase is driven in cortical progenitors starting from E9.5 and reaching full recombination activity before E12.5 (Gorski et al., 2002). After performing IHC in E15.5 brain sections using an anti-BAF155 antibody, a complete loss of BAF155 protein in the pallium of *Baf155*$^{fl/fl}$*;Emx1-Cre* embryos was observed, thus confirming *Baf155* knockout (Figure S1A). The term "BAF155cKO" is used for all subsequent references

to *Baf155*$^{fl/fl}$*;Emx1-Cre* embryos. The BAF155cKO mice were viable, healthy, and fertile and reached adulthood. Although from our previous study we observed that the activation and inactivation of *Baf170* profoundly affect the expression of BAF155 in cortical tissues, the expression of BAF170 is largely preserved in the BAF155cKO cortex (Figure S1A). To confirm that there is no increase in apoptosis, we performed IHC using antibody against cleaved-caspase3. The results indicated that BAF155cKO mice do not show an increase in apoptosis in the cortex, including in the PAX6+ RG cell population (Figure S1B).

BAF155 Controls Expression of a Large Set of PAX6-Target Genes by Potentiating PAX6 Transcriptional Activity

Previous findings indicated that PAX6 interacts with BAF subunits, including BRM, BAF170, and BAF155 in cortical cells (Ninkovic et al., 2013; Tuoc et al., 2013a). To investigate whether the interaction between BAF155 and PAX6 influences PAX6-dependent transcriptional activity, we used a PAX6-dependent reporter vector (pCON/P3) (Epstein et al., 1994; Tuoc and Stoykova, 2008) and primary cortical neural stem cell (NSC) culture from BAF155cKO and control embryos. The NSCs were nucleofected with pCON/P3 plus eGFP plasmids, and the expression level of luciferase was examined by western blot (WB) analysis after 2 days *in vitro* (DIV). We found that without affecting the expression of PAX6, the loss of BAF155 in NSCs led to a significantly reduced level of luciferase as compared with those from control embryos (Figures 2A and 2B). To determine if BAF155 regulates PAX6-dependent transcriptional activity *in vivo*, E13.5 brains of BAF155cKO and control embryos were electroporated with pCON/P3 plus eGFP plasmids. One day post-electroporation, cortical tissue was examined by WB for luciferase expression. Protein quantification revealed that BAF155cKO cortices contained only 23% of the amount of luciferase protein found in the control (Figures 2A and 2B), thus suggesting that BAF155 is required for normal PAX6-dependent transcriptional activity.

To gain further insights into the functional interaction between BAF155 and PAX6, we determined gene expression changes by applying transcriptomic analysis of E15.5 BAF155cKO and PAX6cKO cortices (Figures 2C and 2D). In the PAX6cKO cortex, there were 2,956 down- and 2,415 up-regulated genes, whereas in the BAF155cKO cortex those numbers were 1,179 and 939, respectively (Figures 2C and 2D, Tables S1 and S2, p value < 0.01 & |fold change| > 1.2). Furthermore, we noticed considerable overlap between BAF155- and PAX6-regulated genes, with altered expression (up/down) in the corresponding mutants (Figures 2E and 2F, Table S3). Gene ontology (GO) analysis of the RNA-seq data of the down-regulated genes in PAX6cKO and BAF155cKO (Figures 2G and 2H) revealed that both BAF155 and PAX6 control the expression of genes related to forebrain development, neurogenesis, and neuron differentiation, among others (Figures 2G and 2H, Tables S4 and S5). Taken together, these findings suggested that BAF155 controls the expression of a large set of PAX6-regulated genes, possibly by potentiating PAX6 transcriptional activity.

BAF155 Controls Genesis of Basal Intermediate Progenitors

Earlier studies have identified TF PAX6 as an intrinsic determinant of the RG-cell fate that controls the choice of direct *versus* indirect mode of cortical neurogenesis, the latter depending specifically on bIP production (Georgala et al., 2011; Gotz et al., 1998; Quinn et al., 2006; Sansom et al., 2009; Thakurela et al., 2016; Tuoc et al., 2009, 2013a). In our RNA-seq experiment, the expression of over ten genes with known role in bIP genesis (such as *Eomes/Tbr2, Neurog1, Neurog2, Neurod1, Unc5d, Cxcl12, Sstr2, Pou3f2, Pou3f3, Cux1, Cux2*) was down-regulated not only in PAX6cKO (Figure 3A, Table S1), but also in the BAF155cKO cortex (Figure 3B, Table S2). We then tested whether BAF155 also controls the promoter activity of bIP genes, which are known to be direct targets of PAX6, such as *Ngn2* (Scardigli et al., 2003), *Tbr2, Cux1* (Sansom et al., 2009; Tuoc et al., 2013a). Indeed, we found that the knock down (KD) of BAF155 reduces PAX6-dependent activation of those promoters in the luciferase reporter assay (Figure 3C). Furthermore, we quantitatively studied bIP generation in the BAF155cKO cortex by examining the expression of the bIP marker TBR2 (Hevner et al., 2006), as well as NGN2 and AP2α, both of which label progenitors transitioning between aRGs and bIPs (Arnold et al., 2008; Ochiai et al., 2009; Pinto et al., 2009; Sessa et al., 2008). We found that in BAF155cKO embryos, the number of TBR2+ bIPs and AP2α+/NGN2+ cells (bIPs and aRGs) were substantially diminished (Figures 3D–3G, S2A, and S2B), suggesting that BAF155 cooperates with TF PAX6 to regulate bIP genesis in the developing cerebral cortex.

Ectopic Distribution of Cortical Progenitors in BAF155-Deficient Cortex

Although the total number of TBR2+/AP2α+/NGN2+ bIPs is lower in the BAF155cKO mutant as compared with the control, an extensive ectopic presence of TBR2+/AP2α+/NGN2+ cells (bIPs) was seen in the

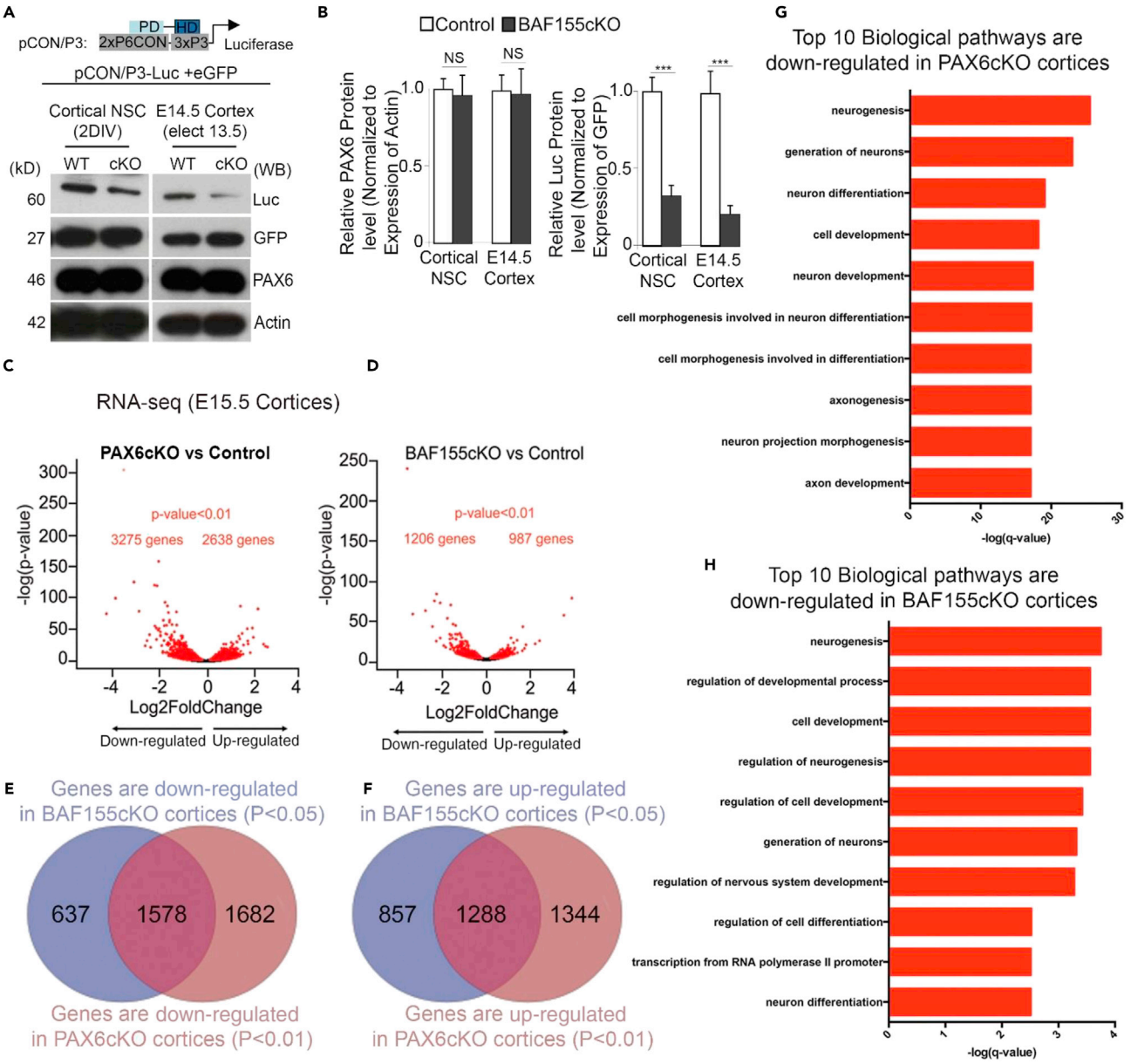

Figure 2. BAF155 and PAX6 Co-regulate Global Gene Expression Program in Developing Cerebral Cortex

(A and B) Luciferase reporter assay was performed using pCON/P3 construct containing PAX6 binding motifs that drives luciferase expression. The construct was transfected to cortical NSCs or electroporated into E13.5 brain, and samples were collected 2 DIV or 1 DPE, respectively, for western blotting (A). In both cases, the loss of BAF155 does not affect the expression of PAX6 (left chart in B). There is, however, a significant reduction of luciferase activity in BAF155cKO compared with control (right chart, B).

(C and D) RNA-seq was performed using cortical samples from E15.5 BAF155cKO and PAX6cKO embryos. Graphs depict the number of both down- and up-regulated genes in BAF155cKO (C) and PAX6cKO (D).

(E and F) The overlap between genes down- (E) and up-regulated (F) in BAF155cKO and PAX6cKO embryos.

(G and H) Gene ontology analysis with the top ten pathways revealed that both BAF155 and PAX6 regulate key genes involved in forebrain development, neurogenesis, and neuron differentiation. Values are presented as Means ± SEMs (***p < 0.001) Abbreviations: NSC, neural stem cell; DIV, days *in vitro*; DPE, days post-electroporation. See also Tables S1, S2, S3, S4, and S5.

intermediate zone (IZ) and cortical plate (CP) (Figures 3D–3G, S2A, and S2B, white arrow). Intrigued by this finding, we next quantified the RG cell populations in the developing pallium by using both nuclear (PAX6, SOX2, AP2**x**) and cytoplasmic (GLAST, BLBP) RG markers (Hartfuss et al., 2001). Interestingly, we found significantly more ectopic RGs in the IZ/CP of the BAF155cKO cortex that are PAX6+ (Figures 4A–4C),

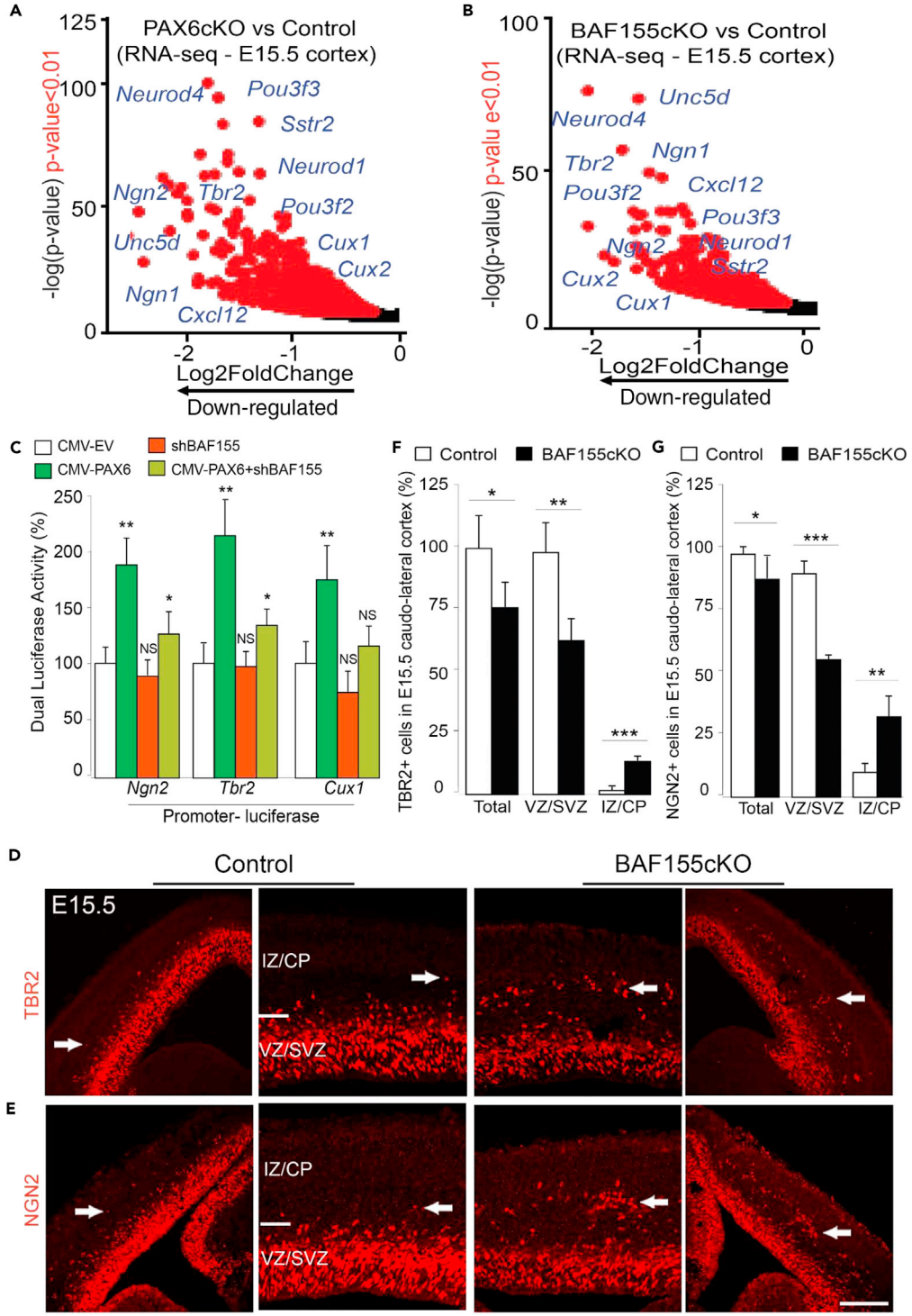

Figure 3. BAF155 Deficiency Leads to a Decreased Number of Basal Intermediate Progenitors in SVZ

(A and B) RNA-seq analysis of samples from E15.5 PAX6cKO (A) and BAF155cKO (B) cortices revealed transcriptional down-regulation of genes with known functions in bIP genesis.

(C) Luciferase reporter assay in Neuro2A cells indicates that BAF155 controls PAX6-dependent activation of bIP lineage-specific gene promoters (*Ngn2, Tbr2, Cux1*).

(D and E) IHC for bIP markers TBR2, NGN2 on coronal sections of E15.5 control (left) and BAF155cKO (right) cortices. Higher magnification is presented in the middle panels.

Figure 3. *Continued*

(F and G) Statistical analysis of the number of TBR2+ (F) and NGN2+ (G) cells in E15.5 cortices revealed diminished numbers of total TBR2+ and NGN2+ cells in the BAF155cKO compared with control.

Note in D and E the presence of TBR2+, NGN2+ cells in ectopic basal locations (white arrows). Values are presented as means ± SEMs (*0.01 < p < 0.05, **0.001 < p < 0.01, ***p < 0.001). Abbreviations: SVZ, subventricular zone; IZ, intermediate zone; bIP, basal intermediate progenitor. Scale bar, 100 μm. See also Figures S2–S5.

SOX2+/GLAST+, and AP2α+/BLBP+ (Figure S2). This visibly enlarged set of PAX6+ and TBR2+ cells in the IZ/CP of the BAF155cKO cortex are cycling progenitors, because many of them are immunoreactive for KI67 as well as BrdU antibody upon 1 hr pulse-labeling (Figure 4D, filled arrows) but negative for NeuN staining (Figure 4D, empty arrows). Some of those RG in the IZ/CP were positive for phosphorylated Vimentin (pVIM, a cytoplasmic marker for dividing RG) and were also labeled with DiI, displaying their clear pia-directed basal process characteristic of bRGs (Figures 4E and 4F, white arrow) (Fietz et al., 2010; Hansen et al., 2010; Wang et al., 2011). Interestingly, the results from our RNA-seq analysis (Figure S3A) indicated that the expression of most of the recently identified bRG-specific genes, such as *Tnc, Ptprz1, Fam107a, and Hopx* (Pollen et al., 2015; Thomsen et al., 2016), was altered in the cortex of PAX6cKO and BAF155cKO mutants. Thus, both TF PAX6- and BAF155-dependent chromatin remodeling seem to play a role in controlling the gene expression program of bRGs.

Reminiscent to reported characteristics of the mouse VZ/SVZ (Hevner et al., 2006) and human oSVZ (Hansen et al., 2010), we observed that the IZ/CP in the BAF155cKO cortex at E15.5 contained PAX6+/SOX2+, NGN2+, and TBR2+ progenitors, which could be cataloged through triple IHC analyses into distinct populations: SOX2+/NGN2+/TBR2+, SOX2+, SOX2+/NGN2+, NGN2+/TBR2+, and TBR2+ cells. Notably, BPs that were immunoreactive only for NGN2 or SOX2/TBR2 were very rare. These findings are suggestive of a sequential expression of TFs during bRGs to bIPs differentiation in the BAF155cKO cortex (Figures S3B–S3D).

To further characterize the abundance of bRGs during the neurogenic phase of cortical development, we quantified the number of PAX6+ cells in the BAF155cKO cortex between E13.5 and E16.5. TAU-1 or TUJ1 immunoreactivity was used to distinguish the boundaries between the VZ/SVZ and IZ/CP (Martinez-Cerdeno et al., 2012) (Figure S4A). We found that the ectopic PAX6+ cells appear in the BAF155cKO cortex from E14.5, 1 day after the preplate splitting known to initiate the formation of cortical layering at E13.5 (Figure S4B). Our analysis revealed that the total number of PAX6+ RGs was not significantly different in the control and BAF155cKO cortices; however, the number of PAX6+ aRGs was strongly diminished, together with a remarkable increase of bRGs in the IZ/CP (Figures 4A–4C).

Earlier studies have established that the mitotic cleavage plane of aRG influences the fate of its progenies (Asami et al., 2011; Estivill-Torrus et al., 2002; Postiglione et al., 2011; Sanada and Tsai, 2005). Given the presence of bRGs in the BAF155cKO cortex, we were curious to know whether BAF155 has a similar role in regulating the mitotic cleavage plane of aRG. We therefore performed a double IHC for pVIM (cytoplasmic marker for dividing RG) and pHH3 (nuclear marker for dividing cells) (Figure 4G). We found that loss of BAF155 resulted in a shift in mitotic cleavage planes from vertical to orientations with reduced angle (Figure 4H). It is particularly interesting to note that in the BAF155cKO cortex, there is a clear increase in the number of aRGs having a horizontal cleavage plane orientation, which is known to predominantly generate bRGs (Asami et al., 2011; Estivill-Torrus et al., 2002; Postiglione et al., 2011). In addition, the expression of many genes, which belong to cleavage plane orientation-related pathways (e.g., mitotic spindle, such as *Par3, Plk1, Eml1, Map4, Dctn1, Arhgef2*), was down-regulated in the PAX6cKO and BAF155cKO cortices in our RNA-seq GO analysis (Table S2, Figure 4I). To ascertain that these findings are progenitor-specific, we created a cortical neuron-specific knockout of BAF155 by using *Nex*-Cre (Goebbels et al., 2006). The selective deletion of BAF155 in post-mitotic neurons did not cause the abnormal distribution of cortical progenitors in the IZ/CP (Figure S4C), indicating that post-mitotic expression of BAF155 plays no demonstrable role in the genesis of BPs.

Taken together, these results indicate that the loss of BAF155 during corticogenesis induces the genesis of basal progenitors with distinct basal processes that express RG and IP molecular markers. These bRGs appear to be generated, at least in part, through a change in the mitotic cleavage plane of aRGs.

Conditional Ablation of BAF155 Has No Significant Effect on Cortical Layer Formation

Given the significant loss of bIPs and ectopic distribution of cortical progenitors in the IZ/CP of the BAF155cKO mutant, we examined if this had any consequence on cortical size and thickness. To this

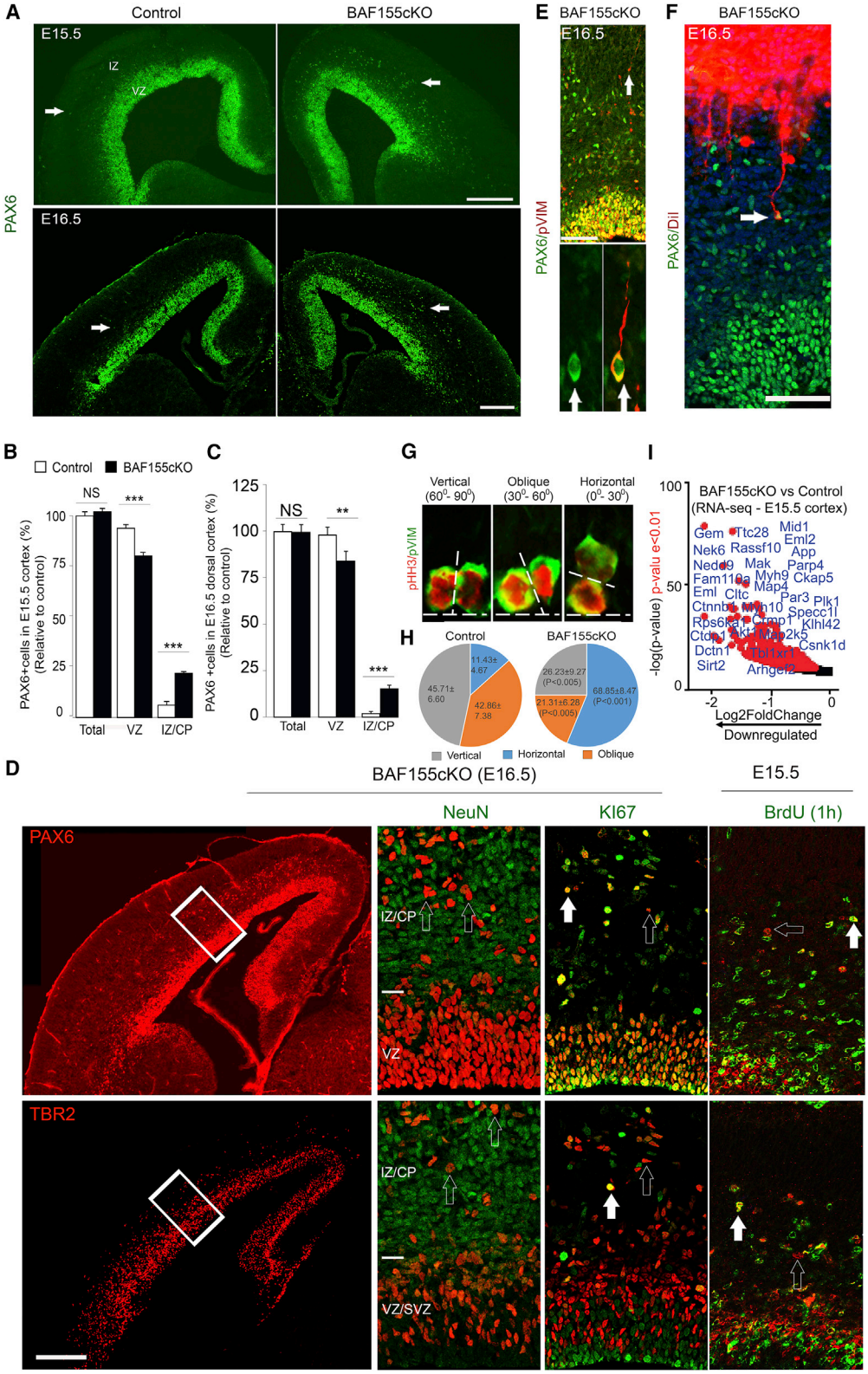

Figure 4. BAF155-Deficient Cortex Displays Increased Number of Basal Radial Glial Progenitors

(A) IHC for RG marker PAX6 on coronal sections of control (left) and BAF155cKO (right) cortices at E15.5 and E16.5. Note the presence of more PAX6+ RG in ectopic basal locations (white arrows) in BAF155 mutant cortices.

Figure 4. *Continued*

(B and C) Statistical analysis of the total number of PAX6+ RG comparing BAF155cKO and control cortices across rostral, medial, and caudal regions at E15.5 (B) and dorsal cortical region at E16.5 (C). Although the total number of PAX6+ RG remains unaffected, a diminished number of PAX6+ RG in the VZ and an increased number of PAX6+ RG in the IZ was found in the BAF155cKO cortex as compared with control.

(D) IHC analysis indicated that these PAX6+, TBR2+ cells are NSCs, as many of them are immunoreactive for KI67 and BrdU (filled arrows) and are negative for NeuN (empty arrows).

(E and F) bRGs with a long basal but missing apical process in the BAF155cKO cortex shows double labeling after IHC with PAX6 and phosphorylated Vimentin (pVIM) antibodies (E) or DiI labeling (F). High magnification of PAX6+/pVIM+ bRG cells (marked by arrow) is shown in the lower panels.

(G and H) To compare RG mitotic cleavage plane orientation in control and BAF155cKO mutants, E15.5 cortices were stained for pVIM and phosphorylated Histone H3 (pHH3) to mark mitotic cells and mitotic chromatin, respectively (G). The observed angle between the cleavage plane and the apical surface of the cortex were grouped into three classes, 60–90° scored as vertical, 30–60° as oblique, and 0–30° as horizontal cell divisions. Note that in the BAF155cKO cortex, there is a shift from vertical to non-vertical divisions (H).

(I) RNA-seq transcriptome profiling between control and BAF155cKO cortices showing down-regulated transcripts, among which numerous genes belong to cleavage plane orientation-related pathways (such as *Par3, Plk1, Eml1, Map4, Dctn1,* and *Arhgef2*).

Values are presented as means ± SEMs (**$0.001 < p < 0.01$, ***$p < 0.001$). Abbreviations: VZ, ventricular zone; IZ, intermediate zone; RG, radial glia; bRG, basal radial glia. Scale bar, 100 μm (A and D), 25 μm (E and F). See also Figures S2, S3, and S5.

end, we performed IHC in coronal sections of E18.5 control and BAF155cKO cortices using antibodies against CTIP2 (marker for early-born neurons/lower layer marker, LL) (Figures S5A–S5C) and SATB2 (marker for late-born neurons/upper layer marker, UL) (Figures S5B and S5C). The results indicated that there is no significant change in the number of both LL and UL neurons in the rostral and caudal regions of the BAF155cKO cortex compared with control (Figures S5A–S5C). Quantifications of Tbr1+ UL and LL neurons at stage P7 in control and BAF155cKO cortex sagittal sections (at medial and lateral levels) did not reveal any significant defects in the layering in BAF155 loss of function (LOF) (Figure S5D). To assess more precisely eventual defects in cortical size and thickness upon deletion of the BAF155 subunit, we employed *ex vivo* the structural magnetic resonance imaging (MRI) approach. The total thickness, size, and surface area of the cerebral cortex were not significantly different between adult (P56) BAF155cKO and control mice at any level (Figures S5E–S5G). Collectively, these findings suggest that, despite the alteration in pool size of bIP (diminished) and bRGs (increased), the BAF155cKO cortex displayed normal surface area and thickness.

Loss of BAF155 or PAX6 Induces Genesis of Basal Progenitors Preferably in Non-Cell-Autonomous Manner

As the loss of BAF155 (Figures 3 and 4) and PAX6 (Asami et al., 2011) triggered the ectopic distribution of cortical progenitors in the IZ, we were interested in determining if BAF155 and PAX6 act within a common genetic pathway in basal progenitor specification. Owing to the severe down-regulation of GLAST expression in the PAX6cKO cortex (Figure S6A), we sought to compare the number of cortical aRGs and bRGs (SOX2+/GLAST+) in the cortex-specific single (BAF155cKO) and double (BAF155, PAX6cKO; dcKO) mutants. The number of SOX2+/GLAST+ aRG in BAF155cKO is similar to that of the control, whereas the additional loss of *Pax6* in dcKO resulted in a significant reduction of this cell population (Figures S5A–S5C). On the other hand, both the BAF155cKO and dcKO cortices showed significantly higher numbers of SOX2+/GLAST+ bRGs in the IZ as compared with the control (Figures S5A–S5C). In addition, we examined the TBR2+ bIP population in mutants, which lost either BAF155 or PAX6 or both at E16.5 (Figures S6B–S6D). Compared with the control, a depleted pool of TBR2+ bIPs was observed in the BAF155cKO cortex and more severely in PAX6cKO mutants. Notably, an almost equal number of TBR2+ bIPs was seen in PAX6cKO and PAX6_BAF155cKO mutants (Figures S6B–S6D). Thus, our data suggested that PAX6 has a lead role, whereas BAF155 acts as a PAX6 cofactor in bIP genesis.

To analyze more directly the role of BAF155 and PAX6 in fate choice of aRG, we performed *in utero* electroporation (IUE) using Cre-ires-eGFP (Hand et al., 2005) plasmid to achieve deletion of either *Baf155* or *Pax6* from aRGs and their progenies in the E13.5 cortex of *Baf155*fl/fl or *Pax6*fl/fl embryos (Figure 5A). The cortical tissue was collected 30 hr after electroporation and immunostained with GFP, SOX2, TBR2 antibodies. Statistical analysis revealed no significant difference in the number of GFP+/SOX2+ aRGs in Cre-injected *Baf155*fl/fl and control hemispheres (Figures 5A and 5B). However, the number of

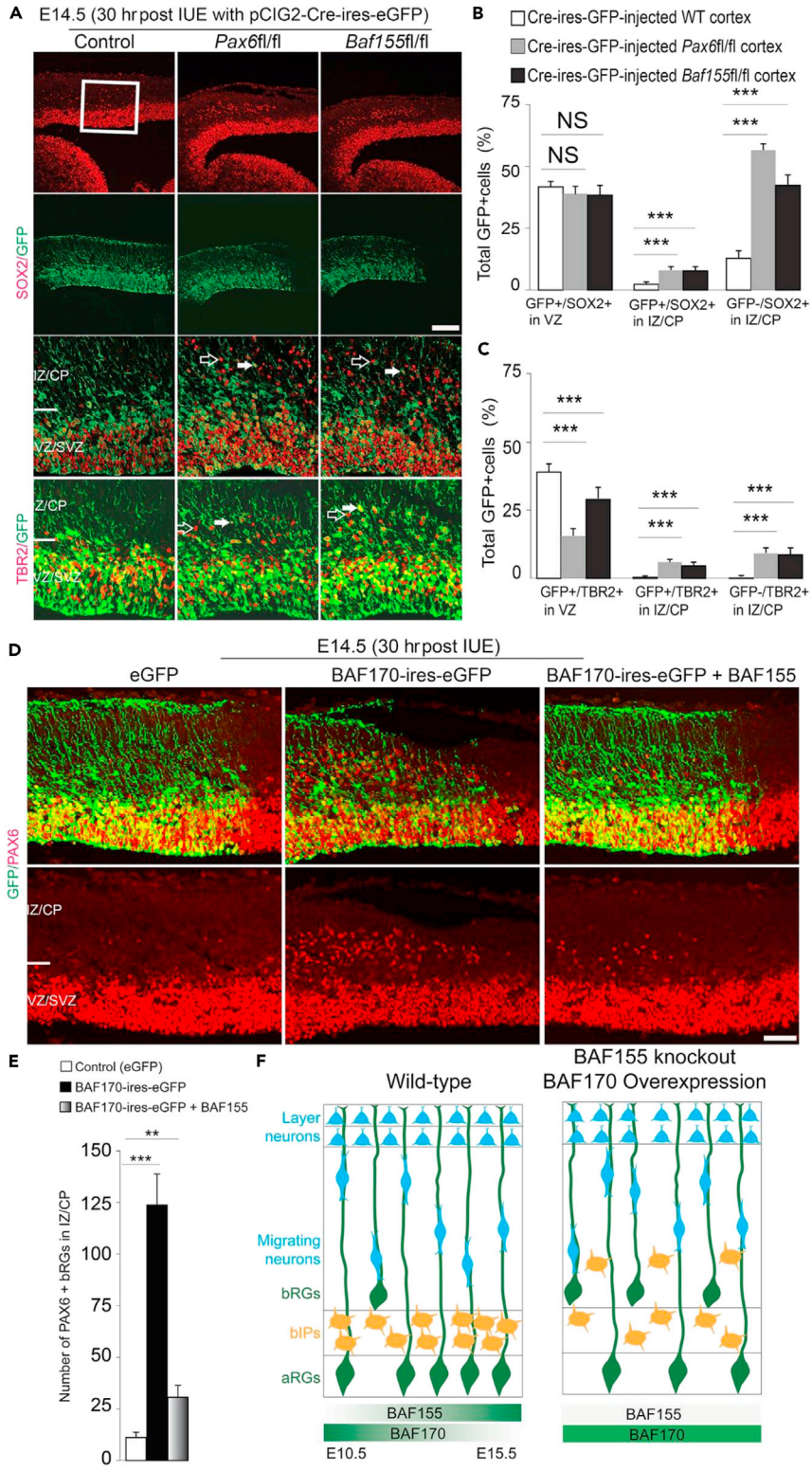

Figure 5. Loss of PAX6 and Competition between BAF155 and BAF170 Promote Genesis of Basal Progenitors Predominantly in Non-Cell-Autonomous Manner

(A–D) Manipulation of endogenous expression level of *Pax6*, *Baf155*, and *Baf170* in aRG via *in utero* electroporation (IUE). E13.5 cortices of WT, *Pax6*fl/fl, or *Baf155*fl/fl embryos were electroporated with the indicated plasmids. Thirty hours

Figure 5. *Continued*

post-electroporation, sections of isolated brains were examined by IHC staining for expression of GFP, RG (SOX2, PAX6), bIPs (TBR2) markers. (B and C) The total number of GFP+ cells in the electroporated cortical areas was used as a reference (as 100%) with which other categories of cells (GFP+/SOX2+, GFP-/SOX2+, and GFP+/TBR2+, GFP-/TBR2+) were compared. Statistical analyses revealed that the loss of PAX6 and BAF155 in IUE experiments led to decrease in the number of GFP+/TBR2+ bIPs in the SVZ, but not GFP+/SOX2+ RG in the VZ, accompanied by an increase in GFP+/TBR2+ and GFP+/SOX2+ basal progenitors in the IZ/CP. Remarkably, the basal progenitors in the IZ/CP were predominantly GFP− (white empty arrows in A) than GFP+ (white filled arrows in A).

(E) Statistical comparisons indicated that overexpression of BAF170, which causes diminished expression of BAF155 (Tuoc et al., 2013a, 2013b), leads also to augmentation of the number of PAX6+ bRGs in the IZ/CP. This phenotype is partially rescued upon co-electroporation with both BAF170/BAF155 expression plasmids.

(F) The scheme illustrates the temporal complementary expression patterns of BAF155 and BAF170 in aRG in early and mid-corticogenesis as well as the effect of BAF155cKO or BAF170 overexpression in BP generation.

Values are presented as means ± SEMs (***$p < 0.001$). Abbreviations: VZ, ventricular zone; SVZ, subventricular zone. Scale bar, 100 μm (A), 25 μm (D). See also Figures S5, S6, and S7.

GFP+/TBR2+ cells (bIP fate) in the SVZ was diminished in *Baf155*-ablated cortices as compared with the control (Figures 5A and 5C), indicating that BAF155 controls the genesis of bIPs in a cell-autonomous manner. As expected, the loss of BAF155 following IUE also led to an increase in the number of progenitors in the IZ/CP (Figure 5A, white filled arrows) consisting of both GFP+/SOX2+ and GFP+/TBR2+ cells (Figures 5B and 5C). These results favor the idea that BAF155 LOF shifts the output of dividing aRGs toward BP production in the IZ rather than the generation of bIPs in the SVZ, a phenotype that is even stronger upon PAX6 LOF (Figures 5B and 5C). Remarkably, more GFP(−) BPs (Figure 5A; white empty arrows) than GFP(+) BPs (Figure 5A; white filled arrows) were detected in the IZ/CP of Cre plasmid-injected *Baf155*fl/fl and *Pax6*fl/fl cortices (Figures 5B and 5C). These results suggest that in contrast to the cell-autonomous effect of both BAF155 and PAX6 on the genesis of SVZ bIPs, these two genes control the genesis of BPs in the IZ/CP preferably in a non-cell-autonomous manner.

Competition between BAF155 and BAF170 Subunit Modulates BP Genesis

Our previous data indicated that the composition of BAF complex in cortical progenitors in terms of stoichiometry of BAF170 and BAF155 subunits influenced bIP production (Tuoc et al., 2013a). We sought to investigate whether such interplay might also affect bRG genesis. We examined the phenotypic consequence of overexpression (OE) of BAF170 by means of IUE, which is known to cause diminished expression of BAF155 (Tuoc et al., 2013a, 2013b). As expected, the activation of BAF170 also resulted in an increased number of PAX6+ bRGs in the IZ in non-cell-autonomous mode as seen in the *Baf155*-ablated cortex (Figures 5D and 5E). To ascertain that this phenotype results specifically from the altered stoichiometry between BAF170 and BAF155 within the BAF complex, we co-electroporated both BAF170/BAF155 expression plasmids into the E14.5 cortex and analyzed cortical phenotype after 30 hr. Remarkably, the phenotype observed upon BAF170 overexpression was partially rescued (Figures 5D and 5E), indicating that the balance between BAF170 and BAF155 plays a crucial role in the genesis of both bIPs and bRGs (Figure 5F) (Tuoc et al., 2013a).

In addition to the cortical phenotype analysis of the above-mentioned mutants (BAF170cKO, BAF170_OE, BAF155cKO), we characterized the cortical phenotypes of BAF155_OE mutants, which express an exogenous BAF155 cDNA together with a Myc tag sequence (BAF155-Myc) (Han et al., 2008; Lee et al., 2007) (Figure S7A). Although the transgenic BAF155-Myc is driven by the ubiquitously active CMV/β-actin promoter, notably, the increased level of BAF155 protein was not observed in entire BAF155_OE embryos (e.g., in the developing heart, but not in lung) (Han et al., 2008; Lee et al., 2007). By applying WB and qPCR analyses to quantify the overexpression level of BAF155 protein and mRNA in the BAF155_OE cortex at E13.5 (Figures S7B–S7D), we found that the *Baf155* mRNA level is highly increased (Figure S7D), whereas the total BAF155 protein level is unaltered in the mutant cortex as compared with the control (Figures S7B and S7C). The IHC analysis indicated that there is no difference in the number and distribution of TBR2+ bIPs and PAX6+ RGs between control and BAF155_OE cortices at E15.5 (Figures 7E and 7F). Furthermore, comparable cortical size was seen in mutants and control at P9 and also at adult stage (Figure 7G).

Together, our data imply that the BAF170 subunit is able to compete with the BAF155 subunit within BAF complexes. Accordingly, the loss of BAF170 in cortex-specific BAF170cKO mutants leads to the incorporation of an additional BAF155 subunit(s) into the BAF complex, causing a dramatic over-production of bIPs.

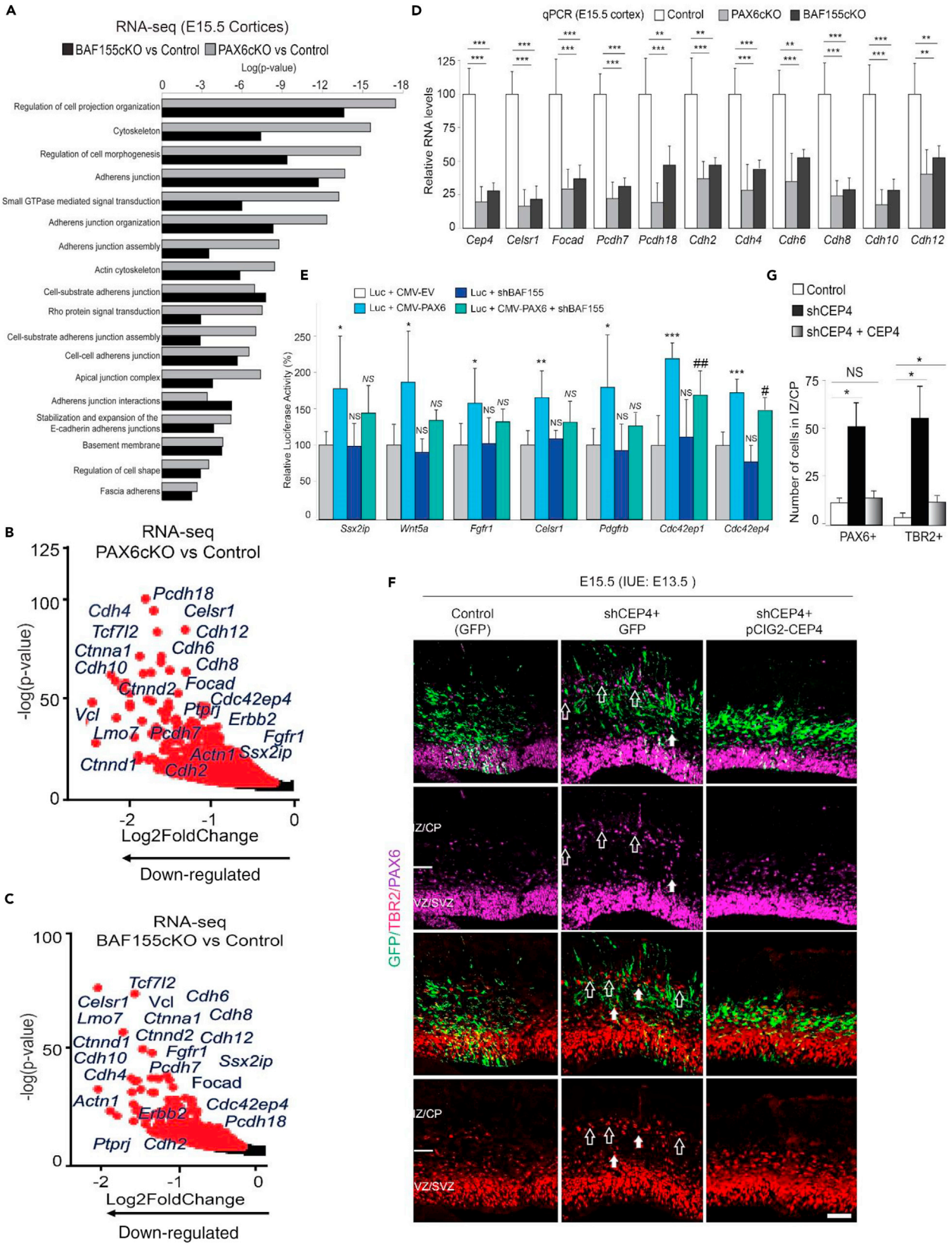
A
RNA-seq (E15.5 Cortices)
BAF155cKO vs Control
PAX6cKO vs Control
Log(p-value)
0 -3 -6 -9 -12 -15 -18
Regulation of cell projection organization
Cytoskeleton
Regulation of cell morphogenesis
Adherens junction
Small GTPase mediated signal transduction
Adherens junction organization
Adherens junction assembly
Actin cytoskeleton
Cell-substrate adherens junction
Rho protein signal transduction
Cell-substrate adherens junction assembly
Cell-cell adherens junction
Apical junction complex
Adherens junction interactions
Stabilization and expansion of the E-cadherin adherens junctions
Basement membrane
Regulation of cell shape
Fascia adherens
B
RNA-seq
PAX6cKO vs Control
-log(p-value)
Log2FoldChange
Down-regulated
Pcdh18
Cdh4
Celsr1
Tcf7l2
Cdh12
Ctnna1
Cdh6
Cdh10
Cdh8
Ctnnd2
Focad
Cdc42ep4
Vcl
Ptprj
Erbb2
Lmo7
Pcdh7
Fgfr1
Actn1
Ssx2ip
Ctnnd1
Cdh2
C
RNA-seq
BAF155cKO vs Control
-log(p-value)
Log2FoldChange
Down-regulated
Tcf7l2
Celsr1
Vcl
Cdh6
Lmo7
Ctnna1
Cdh8
Ctnnd1
Ctnnd2
Cdh12
Cdh10
Fgfr1
Ssx2ip
Pcdh7
Cdh4
Focad
Actn1
Erbb2
Cdc42ep4
Pcdh18
Ptprj
Cdh2
D
qPCR (E15.5 cortex)
Control
PAX6cKO
BAF155cKO
Relative RNA levels
Cep4
Celsr1
Focad
Pcdh7
Pcdh18
Cdh2
Cdh4
Cdh6
Cdh8
Cdh10
Cdh12
E
Luc + CMV-EV
Luc + CMV-PAX6
Luc + shBAF155
Luc + CMV-PAX6 + shBAF155
Relative Luciferase Activity (%)
Ssx2ip
Wnt5a
Fgfr1
Celsr1
Pdgfrb
Cdc42ep1
Cdc42ep4
NS
F
E15.5 (IUE: E13.5)
Control (GFP)
shCEP4+ GFP
shCEP4+ pCIG2-CEP4
GFP/TBR2/PAX6
IZ/CP
VZ/SVZ
G
Control
shCEP4
shCEP4 + CEP4
Number of cells in IZ/CP
NS
PAX6+
TBR2+

Figure 6. BAF155 Regulates Basal Progenitor Genesis through PAX6-Dependent Mechanism Mediated by CEP4

(A) Analysis of gene ontology (GO) from RNA-seq data indicated that many gene pathways that are important for cell-cell interactions were similarly altered in BAF155 and PAX6KO mutants.

(B and C) RNA-seq transcriptome profiling between control and PAX6cKO (B) or BAF155cKO (C) cortices showing down-regulated transcripts, among which numerous genes play important role for cell-cell interaction and cell adhesion.

(D) qPCR confirmation of the selected cell adhesion-related genes down-regulated in PAX6cKO, BAF155cKO cortices at E15.5.

(E) Luciferase reporter assay revealed that PAX6 activates promoter activity of several target genes that are crucial for cell-cell interaction (Luc+CMV-PAX6 condition). Upon silencing of BAF155, this promoter activity tends to reduce (Luc+CMV-PAX6+shBAF155 condition), more significantly for the genes *Cdc42ep1 (Cep1)* and *Cdc42ep4 (Cep4)*.

(F and G) Immunohistochemical (F) and statistical (G) analyses of E15.5 wild-type cortices electroporated with control (GFP), shCEP4 (silencing), or shCEP4+CEP4 (rescue) vectors. Loss of function of CEP4 led to an increase in PAX6+ bRGs and TBR2+ bIPs in the IZ, which are predominantly GFP− (white empty arrow in F) than GFP+ (white filled arrow in F). (G) Statistical analysis of the number of PAX6+ and TBR2+ progenitors in the IZ in the above experiment revealed that there is a significant increase in basal progenitors upon CEP4 silencing compared with the control electroporated cortex. In addition, the co-expression of CEP4 rescued this phenotype.

Values are presented as means ± SEMs ($*/^{\#}0.01 < p < 0.05$, $**/^{\#\#}0.001 < p < 0.01$, $***p < 0.001$). Abbreviations: bRG, basal radial glia; bIP, basal intermediate progenitor; IZ, intermediate zone. Scale bar, 25 μm. See also Figures S8 and S9.

In contrast, overexpression of BAF170 results in competition of BAF170 with BAF155 for occupancy in the BAF complex, leading to a severely depleted bIP pool (Tuoc et al., 2013a) and an increased number of PAX6+ bRGs as observed in the BAF155cKO cortex. BAF170, however, does not substitute for the loss of BAF155 in the BAF155cKO cortex (Figure S1A). Moreover, in the presence of BAF170, exogenous BAF155 molecules are not able to integrate into BAF complexes and the excess BAF155 molecules in the BAF155_OE cortex are possibly degraded post-translationally.

BAF155 Suppresses Progenitor Delamination by Regulating Adherens Junction and Cell-Cell Interaction Machinery

To further investigate the determinants possibly involved in the non-cell-autonomous mechanism by which PAX6 and BAF155 control the genesis of BPs, we examined genes markedly down-regulated in the PAX6cKO and BAF155cKO cortices and having relevance in the maintenance of VZ integrity. The GO analyses of the RNA-seq data showed a significant enrichment of genes involved in cell-cell interaction and cell morphology, including the cell-cell adherens junction (AJ), apical junction complex, basement membrane, actin cytoskeleton, regulation of cell shape, and Rho protein signal transduction, among others (Figures 6A–6C, Tables S4 and S5). For some selected candidates, we also confirmed their down-regulation by qPCR (Figure 6D). To provide additional evidence that loss of BAF155 as well as PAX6 impairs AJ formation, we examined the expression of AJ molecules (ZO1 and α-catenin), which shows a down-regulated expression in our RNA-seq analysis. The expression of these AJ molecules is highly enriched at the apical surface (Figure S8). Consistent with the RNA-seq data, the protein level of ZO1 and α-catenin was apparently lower as revealed by fainter fluorescent intensity in the PAX6cKO, BAF155cKO cortices as compared with the control (Figure S8).

Aiming at identifying target genes of PAX6 and BAF155 that control cell-cell interaction and AJ, we focused on the down-regulated genes from GO terms related to these processes (Figure 6A) in our RNA-seq data for PAX6cKO (Figure 6B) and BAF155cKO cortices (Figure 6C). Moreover, promoters of many genes in these categories, such as *Ssx2ip, Wnt5a, Fgfr1, Celsr1, Cdc42ep1, and Cdc42ep4*, were found to be bound by PAX6 in the previously published PAX6 ChIP-seq data (Xie et al., 2013). Promoter regions of these candidate genes were cloned into vector driving luciferase expression and transiently transfected into Neuro2A cells together with a combination of PAX6-expression and BAF155-silencing vectors. After lysate collection and luminescence quantification, the results from the reporter assay confirmed that compared with the control (in Luc+ CMV-EV condition), PAX6 (in Luc+ CMV-PAX6 condition) significantly regulates the promoter activity of these genes (Figure 6E). However, upon *Baf155* knockdown using a short hairpin RNA (shRNA) construct, the level of luciferase reduced (Luc+ CMV-PAX6+shBAF155 condition), specifically in the case of *Cdc42ep1* and *Cdc42ep4* genes, implying that both PAX6 and BAF155 are required for maintaining the promoter activity of these genes (Figure 6E).

We chose for further functional characterization the two CDC42 effector proteins 1 and 4 (CDC42EP1/CEP1 and CDC42EP4/CEP4), members of the Rho family of guanosine triphosphatases (GTPases), which are known key players in cytoskeletal remodeling acting downstream of CDC42 to induce actin filament organization (Hirsch et al., 2001; Joberty et al., 2001). Because *Cep4* but not *Cep1* is specifically expressed in the E14.5 cortical VZ (Figure S9A) (Visel et al., 2004), we focused on understanding whether *Cep4* is important

for the genesis of BPs. We designed shRNA construct against *Cep4* (Figure S9B) and electroporated it into E13.5 WT cerebral cortices (Figure 6F). Interestingly, 48 hr post-electroporation, knockdown of *Cep4* resulted in an obvious increase in numbers of both PAX6+ bRGs and TBR2+ bIPs in the IZ compared with the control (GFP-only electroporated cortex) (Figures 6F and 6G). Similar to the data from our *in vivo* LOF experiments for BAF155 and PAX6 through IUE, a majority of bIPs and bRGs in *Cep4* shRNA electroporated cortex were GFP(−) cells (Figure 6F, white empty arrow). In addition, co-electroporation of *Cep4* shRNA and pCIG2-CEP4 overexpression plasmid was able to rescue the effect of *Cep4* knockdown (Figures 6E and 6F). Taken together, our findings strongly support the idea that BAF155 controls the genesis of bRGs in a non-cell-autonomous manner, at least in part, by directly regulating PAX6 target genes (such as *Cep4*) involved in cell shape dynamics and cell-cell interaction.

BAF155 Regulates the Expression of Human RG-Specific Genes

Both BAF155 LOF (this study) and PAX6 LOF (Asami et al., 2011) cause ectopic location of basal progenitors in the IZ of the developing cortex. However, although the generation of distinct neuronal identities were unaffected in the BAF155cKO cortex, a lack of PAX6 has been reported to result in an expansion of LL at the expense of UL neurons (Georgala et al., 2011; Gotz et al., 1998; Quinn et al., 2006; Sansom et al., 2009; Thakurela et al., 2016; Tuoc et al., 2009, 2013a). In addition, the analysis of the transcriptome data of BAF155cKO and PAX6cKO cortices indicated that despite the significant overlap in differentially expressed genes, a set of genes appeared to be independently regulated by BAF155 (Figures 2E and 2F).

Recently, evidence has been presented for genes showing specific expression in the RG of the human cortex (hRG) (Lui et al., 2014). Comparing our RNA-seq data of cortical samples from the BAF155cKO mutant with those of Lui et al. (2014), we identified that three such hRG-specific genes, *Foxn4, Lrig3* and *C8orf4*, were up-regulated in BAF155cKO, but not in the PAX6cKO cortex (Figures 7A and 7B). Interestingly, *Foxn4*, although present in the mouse genome, is not expressed in the mouse cortex (Figure S9C) (Visel et al., 2004). To get insight into its function, we generated the *Foxn4* cDNA expression vector (Figure S9D) and performed GOF *in vivo* through IUE into E13.5 WT cerebral cortices. Interestingly, 2 days post-electroporation, we observed increased delamination of both PAX6+ RG and TBR2+ bIPs, giving rise to abundant BP population (Figures 7C and 7D), the majority of which were GFP(−) cells (Figure 7C, white empty arrow). Together, these findings suggest that during mouse cortical development, chromatin remodeler BAF155 seems to suppress the expression of hRG-specific genes (such as *Foxn4*), which otherwise promotes abundant generation of BPs in the primate brain.

DISCUSSION

During cerebral cortex development, glutamatergic neurons are sequentially produced in an inside-out fashion—first the LL neurons followed by UL neurons. The aRGs in the VZ undergo different modes of neurogenesis, either giving rise predominantly to LL neurons (direct neurogenesis) or to UL neurons (indirect neurogenesis) produced by several types of BP descendants located in the SVZ (Gotz and Huttner, 2005; Kriegstein et al., 2006; Leone et al., 2008; Molyneaux et al., 2007; O'Leary et al., 2007; Tuoc et al., 2014). In lissencephalic species, such as mouse, the SVZ is mainly populated by bIPs, which account for the generation of UL neurons and contribute to the radial expansion of the cortex. However, in gyrencephalic species, such as primates and humans, the pool of BPs becomes expanded comprising not only of bIPs but also bRGs, assumed to underlie an exponential increase in neuronal output, expansion and folding of the cortex (Dehay et al., 2015; Fernandez et al., 2016; Florio and Huttner, 2014; Lui et al., 2011; Sun and Hevner, 2014; Taverna et al., 2014; Tuoc et al., 2014). In this study, we have shown data suggesting that the BAF155 subunit of chromatin remodeling BAF complex possibly regulates BP genesis involving PAX6-dependent and PAX6-independent mechanisms.

BAF155 and PAX6 Regulate bRG Genesis by Maintaining Adherens Junction Formation and VZ Integrity

Evidences have been shown that the commitment of the aRG to generate bIP fate occurs upon activation of the expression of PAX6 target genes (*Ngn2, Tbr2*) (Arnold et al., 2008; Sansom et al., 2009; Schuurmans et al., 2004; Sessa et al., 2008; Tuoc et al., 2013a). Similar to the cortical phenotype of the PAX6 LOF mutants, we found that depletion of BAF155 expression caused a diminished bIP pool. In addition, the results

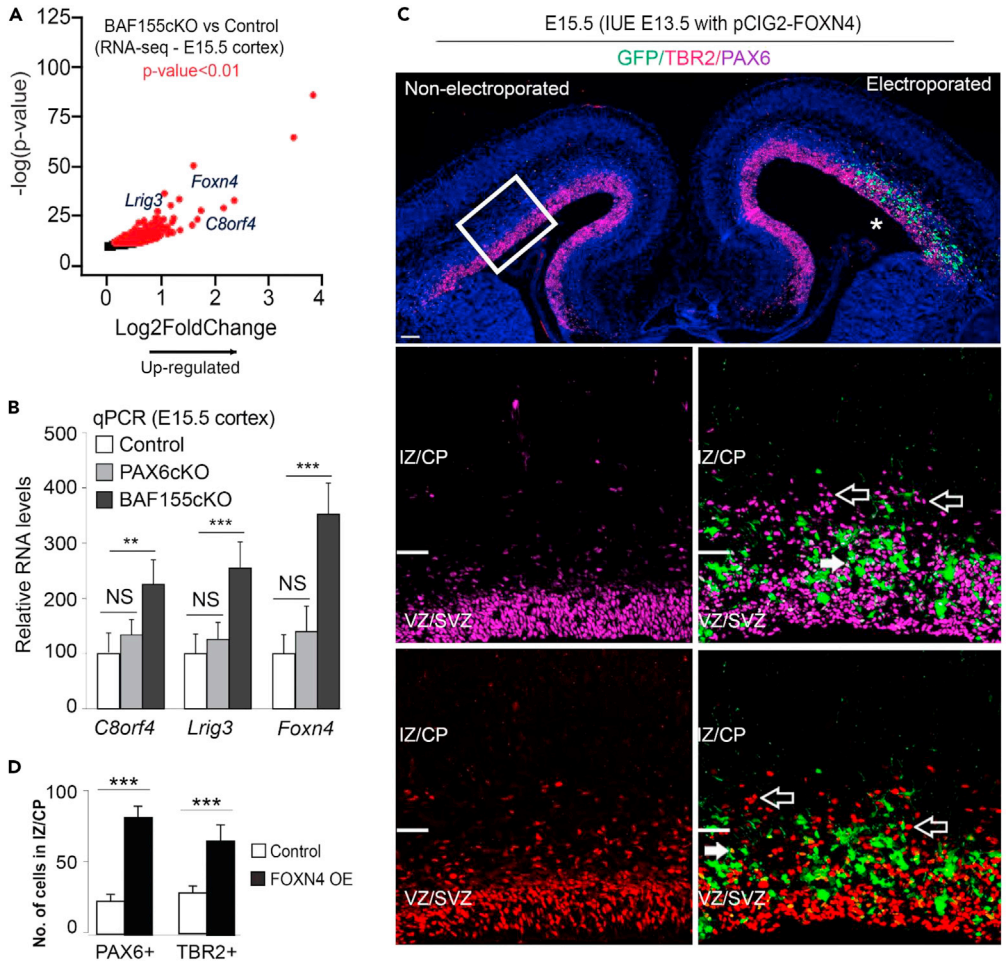

Figure 7. BAF155 Regulates Basal Progenitor Genesis through a PAX6-Independent Mechanism Mediated by FOXN4

(A) RNA-seq transcriptome profiling between control and BAF155cKO cortices showing up-regulated transcripts, among which three genes (*Foxn4, Lrig3* and *C8orf4*) were previously identified as specific to hRGs.

(B) qPCR confirmation of the indicated hRG genes up-regulated in BAF155cKO (but not in PAX6cKO) cortices at E15.5.

(C) Immunohistochemical analysis of E15.5 wild-type cortex electroporated with FOXN4 expression vectors. The FOXN4 GOF resulted in massive delamination of PAX6+ RG and TBR2+ bIPs 48 hr after electroporation compared with the non-injected hemisphere, thus generating abundant populations of bRGs and bIPs in the IZ. Notably, the majority of these basal progenitors were GFP− (white empty arrow) than GFP+ (white filled arrow).

(D) Statistical analysis of the number of PAX6+ and TBR2+ progenitors in the IZ in the same experiment revealed that there is a significant increase in basal progenitors upon FOXN4 GOF compared with the non-electroporated (control) cortex.

Values are presented as Mean ± SEMs (**0.001 < p < 0.01, ***p < 0.001). Abbreviations: VZ, ventricular zone; IZ, intermediate zone; RG, radial glia; bRG, basal radial glia; bIP, basal intermediate progenitor; hRG, human radial glia; GOF, gain of function. Scale bar, 100 μm. See also Figure S9.

from the reporter assay indicate that BAF155 is needed for the activation of PAX6-dependent transcription in cortical progenitors. Furthermore, the RNA sequencing of BAF155cKO and PAX6cKO cortices indicated a significant overlap between differentially expressed (up- or down-regulated) genes in both mutants. Together, these data implicate a possible existence of a link between the PAX6-dependent transcriptional control of bIP genesis and BAF155-dependent chromatin remodeling. However, additional confirmatory experiments (such as ChIP-seq for PAX6, BAF155, epigenetic marks) will be necessary to get a deeper insight into the mechanism of interaction between these two factors.

The loss of PAX6 results in a reduction in the expression of cell adhesion proteins (Asami et al., 2011; Stoykova et al., 1997) known to trigger detachment of aRG from the apical VZ surface to ectopic basal location and

displaying bRG identity (Asami et al., 2011). Similarly, in the BAF155cKO cortex we found an increased frequency of progenitor delamination from the VZ and a significant down-regulation of the expression of genes regulating cell adhesion and AJ. In the ferret developing cortex, a substantial reduction of *Cdh1* expression, alongside change in the orientation of aRG mitotic division plane, resulted in the generation of pioneer bRGs, highlighting the significance of aRG delamination for bRG genesis (Martinez-Martinez et al., 2016). It is plausible therefore to suggest that both BAF155 and PAX6 could be also involved in the regulation of cell adhesion and AJ formation contributing to anchor aRG in the VZ. Although the sustained expression of PAX6 in bIPs in the mouse cortex resulted in a primate-like mode of generation of bRGs suggesting that PAX6 alone is able to reprogram bIPs to bRGs (Wong et al., 2015), our findings highlight an additional role of TF PAX6 in regulating aRG delamination through cell adhesion.

Another interesting finding was that the majority of bRGs found both in the BAF155 and PAX6 LOF cortices seem to arise through non-cell-autonomous mechanism. Upon loss of BAF155 and PAX6, we observed a down-regulation of the expression of CEP4, a CDC42 effector protein, which is specifically expressed in the VZ during corticogenesis. Indeed, we found that BAF155 directly regulates the expression of *Cep4* in a PAX6-dependent manner and that the loss of CEP4 function causes delamination of progenitors in a predominantly non-cell-autonomous manner. Being a multifaceted regulator of cellular signaling, the Rho GTPase CDC42 activates Par complex that maintains the apico-basal polarity of aRG and AJ formation in the developing cortex, thereby regulating apical vs basal fate of the progenitors (Cappello et al., 2006). It is therefore tempting to speculate that CEP4 likely regulates key components of the AJ, cell-cell interaction, and signaling machineries. Although further experiments are needed to study the underlying mechanisms, these results suggest that CEP4 has a role in progenitor delamination participating either directly or through its interaction with CDC42.

Dynamic Expression of BAF155 and BAF170 Has a Functional Relevance in BP Genesis during Cortical Development

During cortical development, both BAF155 and BAF170 are detectable in the progenitor cells of the VZ; however, they show temporal complementary expression patterns (Figures 1 and 5F) (Tuoc et al., 2013a). The expression of BAF155 in aRG peaks at mid-corticogenesis (E15.5-E16.5), whereas a higher level of BAF170 is found in early corticogenesis (E10.5-E13.5). The results presented here suggest that the expression dynamics of the chromatin remodeling subunits BAF155 and BAF170 have a functional relevance in the temporal genesis of BPs during cortical development (Figure 5F).

We have shown previously that TF PAX6 interacts with both BAF155 and BAF170, the latter recruiting REST-corepressor complexes to promoters of PAX6 target genes involved in specification of bIPs (Tuoc et al., 2013a). Loss of BAF170 leads to replacement of BAF170 by an additional BAF155 subunit, elimination of the REST-co-repressor complex, and induction of a euchromatin state that relieves the repression of PAX6 target genes involved in bIP specification. Thus, the biological outcome of BAF subunit exchange is a heterochronic, premature expression of genes that specify bIPs. Conversely, over-expression of BAF170 results in competition with BAF155 for occupancy of the BAF complex that leads (opposite to the BAF170 LOF condition) to an increase of bIP generation. In agreement with these findings, we showed in this study that the loss of BAF155 causes repression of PAX6 target genes involved in bIP specification likely inducing a heterochromatin state on their regulatory regions (Figure 3C).

In addition to the effect on bIP generation, the balance between BAF170 and BAF155 within the BAF complex in cortical progenitors is also essential for bRG genesis. Accordingly, loss of BAF155 achieved by either knockout of BAF155 or overexpression of BAF170 causes delamination of aRG to generate bRGs. Taken together, the results suggest that changes in the equilibrium between BAF170 and BAF155 in aRG result in chromatin re-arrangement on the genomic loci of PAX6 target genes, which are important for bIP specification and delamination of progenitors.

Delamination of aRG Mediated by BAF155 Might Be Relevant for the Expansion of bRGs in the Developing Cortex during Evolution

Since the primate and human cortex contain an expanded population of BPs (Fietz et al., 2010; Hansen et al., 2010; Kelava et al., 2012; Lukaszewicz et al., 2005), we were intrigued to examine whether non-cell-autonomous mechanism of progenitor delamination, as discovered in this study, has acquired evolutionary significance. Interestingly, the transcriptional up-regulation of the expression of *Foxn4,*

Lrig3, and *C8orf4* in BAF155cKO mutants as reported here were previously shown as hRG-specific markers (Lui et al., 2014). Among these genes, we focused on understanding the role of FOXN4, a TF with a known role in the determination of cell fate in retinal progenitor cells (Li et al., 2004). By using the *in vivo* GOF approach, we showed that overexpression of FOXN4 results in a massive progenitor delamination and abundant generation of both bRGs and bIPs (Figure 7) in a non-cell-autonomous manner. Interestingly, a strikingly similar phenotype was previously reported upon overexpression of PDGFRb, another hRG-specific marker (Lui et al., 2014). Together, these findings suggest that, in addition to PAX6-dependent regulation of gene expression, BAF155 appears to control BP genesis independent of PAX6 through regulation of hRG genes, such as *Foxn4*. It would be interesting in future studies to investigate the homology of BAF155 and PAX6 proteins in mouse and human brain, e.g., in amino acid sequences, their species-specific isoforms, and their dynamic expression pattern during corticogenesis, and how such differences can lead to changes in the abundance of bRGs in primates.

In summary, our data revealed the significance of the interaction between the chromatin remodeling BAF complex and transcriptional machinery in the context of progenitor fate choice and basal progenitor genesis during cortical development. Both BAF155 and PAX6 control the AJ formation between the aRG at the ventricular surface, part of which mechanism is directly dependent on CEP4 that acts downstream of both factors. Furthermore, through the regulation of hRG-specific genes, such as *Foxn4*, the BAF155 chromatin remodeling subunit seems to exert a PAX6-independent role in progenitor delamination and bRG genesis that might have acquired evolutionary significance during cortical development.

METHODS

All methods can be found in the accompanying Transparent Methods supplemental file.

DATA AND SOFTWARE AVAILABILITY

The accession number for the RNAseq data reported in this study is GEO:GSE106711.

SUPPLEMENTAL INFORMATION

Supplemental Information includes Transparent Methods, nine figures, and six tables and can be found with this article online at https://doi.org/10.1016/j.isci.2018.05.014.

ACKNOWLEDGMENTS

We acknowledge T. Huttanus and H. Fett for their expert animal care and support. We thank A. Messing, A. Nave, and K. Jones for providing reagents. This work was supported by Research Program, Faculty of Medicine, Georg-August-University Goettingen (T.T.), TU432/1-1, TU432/3-1 DFG grants (T.T.), Schram-Stiftung (T.T.), and DFG-CNMPB (T.T., J.F.S., A.S., A.F.).

AUTHOR CONTRIBUTIONS

R.N., L.P., P.A.U., G.S., R.C.H., A.S., and T.T. characterized the phenotype of BAF155cKO and dcKO mutants; R.N. performed shCEP4, CEP4, and FOXN4 overexpression *in vivo*; R.N. and A.B.T. carried out cell division analysis; T.W., R.N., and J.F. contributed to MRI; R.N. and K.A.K. performed luciferase assay; C.K., S.B., R.N., and A.F. contributed to RNA-seq, analysis of genome-wide data; T.T., L.P., G.S., and J.R. carried out shBAF155, BAF155_OE, shPAX6, BAF170 overexpression *in vivo*; J.F.S., A.S., U.T., and R.H.S. provided transgenic lines and research tools and contributed to discussions. A part of the project was performed in the Stoykova laboratory. T.T. conceived the study.

DECLARATION OF INTERESTS

The authors declare no competing financial interests.

Received: February 8, 2018
Revised: April 22, 2018
Accepted: May 18, 2018
Published: June 29, 2018

REFERENCES

Arnold, S.J., Huang, G.J., Cheung, A.F., Era, T., Nishikawa, S., Bikoff, E.K., Molnar, Z., Robertson, E.J., and Groszer, M. (2008). The T-box transcription factor Eomes/Tbr2 regulates neurogenesis in the cortical subventricular zone. Genes Dev. *22*, 2479–2484.

Asami, M., Pilz, G.A., Ninkovic, J., Godinho, L., Schroeder, T., Huttner, W.B., and Gotz, M. (2011). The role of Pax6 in regulating the orientation and mode of cell division of progenitors in the mouse cerebral cortex. Development *138*, 5067–5078.

Bachmann, C., Nguyen, H., Rosenbusch, J., Pham, L., Rabe, T., Patwa, M., Sokpor, G., Seong, R.H., Ashery-Padan, R., Mansouri, A., et al. (2016). mSWI/SNF (BAF) complexes are indispensable for the neurogenesis and development of embryonic olfactory epithelium. PLoS Genet. *12*, e1006274.

Betizeau, M., Cortay, V., Patti, D., Pfister, S., Gautier, E., Bellemin-Menard, A., Afanassieff, M., Huissoud, C., Douglas, R.J., Kennedy, H., et al. (2013). Precursor diversity and complexity of lineage relationships in the outer subventricular zone of the primate. Neuron *80*, 442–457.

Borrell, V., and Gotz, M. (2014). Role of radial glial cells in cerebral cortex folding. Curr. Opin. Neurobiol. *27*, 39–46.

Cappello, S., Attardo, A., Wu, X., Iwasato, T., Itohara, S., Wilsch-Bräuninger, M., Eilken, H.M., Rieger, M.A., Schroeder, T.T., Huttner, W.B., Brakebusch, C., and Götz, M. (2006). The Rho-GTPase cdc42 regulates neural progenitor fate at the apical surface. Nat. Neurosci. *9*, 1099–1107.

Choi, J., Ko, M., Jeon, S., Jeon, Y., Park, K., Lee, C., Lee, H., and Seong, R.H. (2012). The SWI/SNF-like BAF complex is essential for early B cell development. J. Immunol. *188*, 3791–3803.

Dehay, C., Kennedy, H., and Kosik, K.S. (2015). The outer subventricular zone and primate-specific cortical complexification. Neuron *85*, 683–694.

Epstein, J., Cai, J., Glaser, T., Jepeal, L., and Maas, R. (1994). Identification of a Pax paired domain recognition sequence and evidence for DNA-dependent conformational changes. J. Biol. Chem. *269*, 8355–8361.

Estivill-Torrus, G., Pearson, H., van Heyningen, V., Price, D.J., and Rashbass, P. (2002). Pax6 is required to regulate the cell cycle and the rate of progression from symmetrical to asymmetrical division in mammalian cortical progenitors. Development *129*, 455–466.

Fernandez, V., Llinares-Benadero, C., and Borrell, V. (2016). Cerebral cortex expansion and folding: what have we learned? EMBO J. *35*, 1021–1044.

Fietz, S.A., Kelava, I., Vogt, J., Wilsch-Brauninger, M., Stenzel, D., Fish, J.L., Corbeil, D., Riehn, A., Distler, W., Nitsch, R., et al. (2010). OSVZ progenitors of human and ferret neocortex are epithelial-like and expand by integrin signaling. Nat. Neurosci. *13*, 690–699.

Florio, M., and Huttner, W.B. (2014). Neural progenitors, neurogenesis and the evolution of the neocortex. Development *141*, 2182–2194.

Georgala, P.A., Manuel, M., and Price, D.J. (2011). The generation of superficial cortical layers is regulated by levels of the transcription factor Pax6. Cereb. Cortex *21*, 81–94.

Goebbels, S., Bormuth, I., Bode, U., Hermanson, O., Schwab, M.H., and Nave, K.A. (2006). Genetic targeting of principal neurons in neocortex and hippocampus of NEX-Cre mice. Genesis *44*, 611–621.

Gorski, J.A., Talley, T., Qiu, M., Puelles, L., Rubenstein, J.L., and Jones, K.R. (2002). Cortical excitatory neurons and glia, but not GABAergic neurons, are produced in the Emx1-expressing lineage. J. Neurosci. *22*, 6309–6314.

Gotz, M., and Huttner, W.B. (2005). The cell biology of neurogenesis. Nat. Rev. Mol. Cell Biol. *6*, 777–788.

Gotz, M., Stoykova, A., and Gruss, P. (1998). Pax6 controls radial glia differentiation in the cerebral cortex. Neuron *21*, 1031–1044.

Han, D., Jeon, S., Sohn, D.H., Lee, C., Ahn, S., Kim, W.K., Chung, H., and Seong, R.H. (2008). SRG3, a core component of mouse SWI/SNF complex, is essential for extra-embryonic vascular development. Dev. Biol. *315*, 136–146.

Hand, R., Bortone, D., Mattar, P., Nguyen, L., Heng, J.I., Guerrier, S., Boutt, E., Peters, E., Barnes, A.P., Parras, C., et al. (2005). Phosphorylation of Neurogenin2 specifies the migration properties and the dendritic morphology of pyramidal neurons in the neocortex. Neuron *48*, 45–62.

Hansen, D.V., Lui, J.H., Parker, P.R., and Kriegstein, A.R. (2010). Neurogenic radial glia in the outer subventricular zone of human neocortex. Nature *464*, 554–561.

Hartfuss, E., Galli, R., Heins, N., and Gotz, M. (2001). Characterization of CNS precursor subtypes and radial glia. Dev. Biol. *229*, 15–30.

Hevner, R.F., Hodge, R.D., Daza, R.A., and Englund, C. (2006). Transcription factors in glutamatergic neurogenesis: conserved programs in neocortex, cerebellum, and adult hippocampus. Neurosci. Res. *55*, 223–233.

Hirsch, D.S., Pirone, D.M., and Burbelo, P.D. (2001). A new family of Cdc42 effector proteins, CEPs, function in fibroblast and epithelial cell shape changes. J. Biol. Chem. *276*, 875–883.

Joberty, G., Perlungher, R.R., Sheffield, P.J., Kinoshita, M., Noda, M., Haystead, T., and Macara, I.G. (2001). Borg proteins control septin organization and are negatively regulated by Cdc42. Nat. Cell Biol. *3*, 861–866.

Kelava, I., Reillo, I., Murayama, A.Y., Kalinka, A.T., Stenzel, D., Tomancak, P., Matsuzaki, F., Lebrand, C., Sasaki, E., Schwamborn, J.C., et al. (2012). Abundant occurrence of basal radial glia in the subventricular zone of embryonic neocortex of a lissencephalic primate, the common marmoset *Callithrix jacchus*. Cereb. Cortex *22*, 469–481.

Kriegstein, A., Noctor, S., and Martinez-Cerdeno, V. (2006). Patterns of neural stem and progenitor cell division may underlie evolutionary cortical expansion. Nat. Rev. Neurosci. *7*, 883–890.

Lee, Y.S., Sohn, D.H., Han, D., Lee, H.W., Seong, R.H., and Kim, J.B. (2007). Chromatin remodeling complex interacts with ADD1/SREBP1c to mediate insulin-dependent regulation of gene expression. Mol. Cell. Biol. *27*, 438–452.

Leone, D.P., Srinivasan, K., Chen, B., Alcamo, E., and McConnell, S.K. (2008). The determination of projection neuron identity in the developing cerebral cortex. Curr. Opin. Neurobiol. *18*, 28–35.

Li, S., Mo, Z., Yang, X., Price, S.M., Shen, M.M., and Xiang, M. (2004). Foxn4 controls the genesis of amacrine and horizontal cells by retinal progenitors. Neuron *43*, 795–807.

Lui, J.H., Hansen, D.V., and Kriegstein, A.R. (2011). Development and evolution of the human neocortex. Cell *146*, 18–36.

Lui, J.H., Nowakowski, T.J., Pollen, A.A., Javaherian, A., Kriegstein, A.R., and Oldham, M.C. (2014). Radial glia require PDGFD-PDGFRbeta signalling in human but not mouse neocortex. Nature *515*, 264–268.

Lukaszewicz, A., Savatier, P., Cortay, V., Giroud, P., Huissoud, C., Berland, M., Kennedy, H., and Dehay, C. (2005). G1 phase regulation, area-specific cell cycle control, and cytoarchitectonics in the primate cortex. Neuron *47*, 353–364.

Martinez-Cerdeno, V., Cunningham, C.L., Camacho, J., Antczak, J.L., Prakash, A.N., Cziep, M.E., Walker, A.I., and Noctor, S.C. (2012). Comparative analysis of the subventricular zone in rat, ferret and macaque: evidence for an outer subventricular zone in rodents. PLoS One *7*, e30178.

Martinez-Martinez, M.A., De Juan Romero, C., Fernandez, V., Cardenas, A., Gotz, M., and Borrell, V. (2016). A restricted period for formation of outer subventricular zone defined by Cdh1 and Trnp1 levels. Nat. Commun. *7*, 11812.

Molyneaux, B.J., Arlotta, P., Menezes, J.R., and Macklis, J.D. (2007). Neuronal subtype specification in the cerebral cortex. Nat. Rev. Neurosci. *8*, 427–437.

Ninkovic, J., Steiner-Mezzadri, A., Jawerka, M., Akinci, U., Masserdotti, G., Petricca, S., Fischer, J., von Holst, A., Beckers, J., Lie, C.D., et al. (2013). The BAF complex interacts with Pax6 in adult neural progenitors to establish a Neurogenic cross-regulatory transcriptional network. Cell Stem Cell *13*, 403–418.

O'Leary, D.D., Chou, S.J., and Sahara, S. (2007). Area patterning of the mammalian cortex. Neuron *56*, 252–269.

Ochiai, W., Nakatani, S., Takahara, T., Kainuma, M., Masaoka, M., Minobe, S., Namihira, M., Nakashima, K., Sakakibara, A., Ogawa, M., et al. (2009). Periventricular notch activation and asymmetric Ngn2 and Tbr2 expression in pair-generated neocortical daughter cells. Mol. Cell Neurosci. *40*, 225–233.

Pinto, L., Drechsel, D., Schmid, M.T., Ninkovic, J., Irmler, M., Brill, M.S., Restani, L., Gianfranceschi, L., Cerri, C., Weber, S.N., et al. (2009). AP2gamma regulates basal progenitor fate in a region- and layer-specific manner in the developing cortex. Nat. Neurosci. *12*, 1229–1237.

Pollen, A.A., Nowakowski, T.J., Chen, J., Retallack, H., Sandoval-Espinosa, C., Nicholas, C.R., Shuga, J., Liu, S.J., Oldham, M.C., Diaz, A., et al. (2015). Molecular identity of human outer radial glia during cortical development. Cell *163*, 55–67.

Postiglione, M.P., Juschke, C., Xie, Y., Haas, G.A., Charalambous, C., and Knoblich, J.A. (2011). Mouse inscuteable induces apical-basal spindle orientation to facilitate intermediate progenitor generation in the developing neocortex. Neuron *72*, 269–284.

Quinn, J.C., Molinek, M., Martynoga, B.S., Zaki, P.A., Faedo, A., Bulfone, A., Hevner, R.F., West, J.D., and Price, D.J. (2006). Pax6 controls cerebral cortical cell number by regulating exit from the cell cycle and specifies cortical cell identity by a cell autonomous mechanism. Dev. Biol. *22*, *22*.

Sanada, K., and Tsai, L.H. (2005). G protein betagamma subunits and AGS3 control spindle orientation and asymmetric cell fate of cerebral cortical progenitors. Cell *122*, 119–131.

Sansom, S.N., Griffiths, D.S., Faedo, A., Kleinjan, D.J., Ruan, Y., Smith, J., van Heyningen, V., Rubenstein, J.L., and Livesey, F.J. (2009). The level of the transcription factor Pax6 is essential for controlling the balance between neural stem cell self-renewal and neurogenesis. PLoS Genet. *5*, e1000511.

Scardigli, R., Baumer, N., Gruss, P., Guillemot, F., and Le Roux, I. (2003). Direct and concentration-dependent regulation of the proneural gene Neurogenin2 by Pax6. Development *130*, 3269–3281.

Schuurmans, C., Armant, O., Nieto, M., Stenman, J.M., Britz, O., Klenin, N., Brown, C., Langevin, L.M., Seibt, J., Tang, H., et al. (2004). Sequential phases of cortical specification involve Neurogenin-dependent and -independent pathways. EMBO J. *23*, 2892–2902.

Sessa, A., Mao, C.A., Hadjantonakis, A.K., Klein, W.H., and Broccoli, V. (2008). Tbr2 directs conversion of radial glia into basal precursors and guides neuronal amplification by indirect neurogenesis in the developing neocortex. Neuron *60*, 56–69.

Stoykova, A., Gotz, M., Gruss, P., and Price, J. (1997). Pax6-dependent regulation of adhesive patterning, R-cadherin expression and boundary formation in developing forebrain. Development *124*, 3765–3777.

Sun, T., and Hevner, R.F. (2014). Growth and folding of the mammalian cerebral cortex: from molecules to malformations. Nat. Rev. Neurosci. *15*, 217–232.

Taverna, E., Gotz, M., and Huttner, W.B. (2014). The cell biology of neurogenesis: toward an understanding of the development and evolution of the neocortex. Annu. Rev. Cell Dev. Biol. *30*, 465–502.

Thakurela, S., Tiwari, N., Schick, S., Garding, A., Ivanek, R., Berninger, B., and Tiwari, V.K. (2016). Mapping gene regulatory circuitry of Pax6 during neurogenesis. Cell Discov. *2*, 15045.

Thomsen, E.R., Mich, J.K., Yao, Z.Z., Hodge, R.D., Doyle, A.M., Jang, S.M., Shehata, S.I., Nelson, A.M., Shapovalova, N.V., Levi, B.P., et al. (2016). Fixed single-cell transcriptomic characterization of human radial glial diversity. Nat. Methods *13*, 87–93.

Tuoc, T.C., Boretius, S., Sansom, S.N., Pitulescu, M.E., Frahm, J., Livesey, F.J., and Stoykova, A. (2013a). Chromatin regulation by BAF170 controls cerebral cortical size and thickness. Developmental Cell *25*, 256–269.

Tuoc, T.C., Narayanan, R., and Stoykova, A. (2013b). BAF chromatin remodeling complex: cortical size regulation and beyond. Cell Cycle *12*, 2953–2959.

Tuoc, T.C., Pavlakis, E., Tylkowski, M.A., and Stoykova, A. (2014). Control of cerebral size and thickness. Cell Mol. Life Sci. *71*, 3199–3218.

Tuoc, T.C., Radyushkin, K., Tonchev, A.B., Pinon, M.C., Ashery-Padan, R., Molnar, Z., Davidoff, M.S., and Stoykova, A. (2009). Selective cortical layering abnormalities and behavioral deficits in cortex-specific Pax6 knock-out mice. J. Neurosci. *29*, 8335–8349.

Tuoc, T.C., and Stoykova, A. (2008). Trim11 modulates the function of neurogenic transcription factor Pax6 through ubiquitin-proteosome system. Genes Dev. *22*, 1972–1986.

Visel, A., Thaller, C., and Eichele, G. (2004). GenePaint.org: an atlas of gene expression patterns in the mouse embryo. Nucleic Acids Res. *32*, D552–D556.

Wang, X., Tsai, J.W., LaMonica, B., and Kriegstein, A.R. (2011). A new subtype of progenitor cell in the mouse embryonic neocortex. Nat. Neurosci. *14*, 555–561.

Wong, F.K., Fei, J.F., Mora-Bermudez, F., Taverna, E., Haffner, C., Fu, J., Anastassiadis, K., Stewart, A.F., and Huttner, W.B. (2015). Sustained Pax6 Expression generates primate-like basal radial glia in developing mouse neocortex. PLoS Biol. *13*, e1002217.

Xie, Q., Yang, Y., Huang, J., Ninkovic, J., Walcher, T., Wolf, L., Vitenzon, A., Zheng, D., Gotz, M., Beebe, D.C., et al. (2013). Pax6 interactions with chromatin and identification of its novel direct target genes in lens and forebrain. PLoS One *8*, e54507.

ISCI, Volume *4*

Supplemental Information

Chromatin Remodeling BAF155 Subunit Regulates the Genesis of Basal Progenitors in Developing Cortex

Ramanathan Narayanan, Linh Pham, Cemil Kerimoglu, Takashi Watanabe, Ricardo Castro Hernandez, Godwin Sokpor, Pauline Antonie Ulmke, Kamila A. Kiszka, Anton B. Tonchev, Joachim Rosenbusch, Rho H. Seong, Ulrike Teichmann, Jens Frahm, Andre Fischer, Stefan Bonn, Anastassia Stoykova, Jochen F. Staiger, and Tran Tuoc

SUPPLEMENTAL INFORMATION

SUPPLEMENTAL DATA

Figure S1

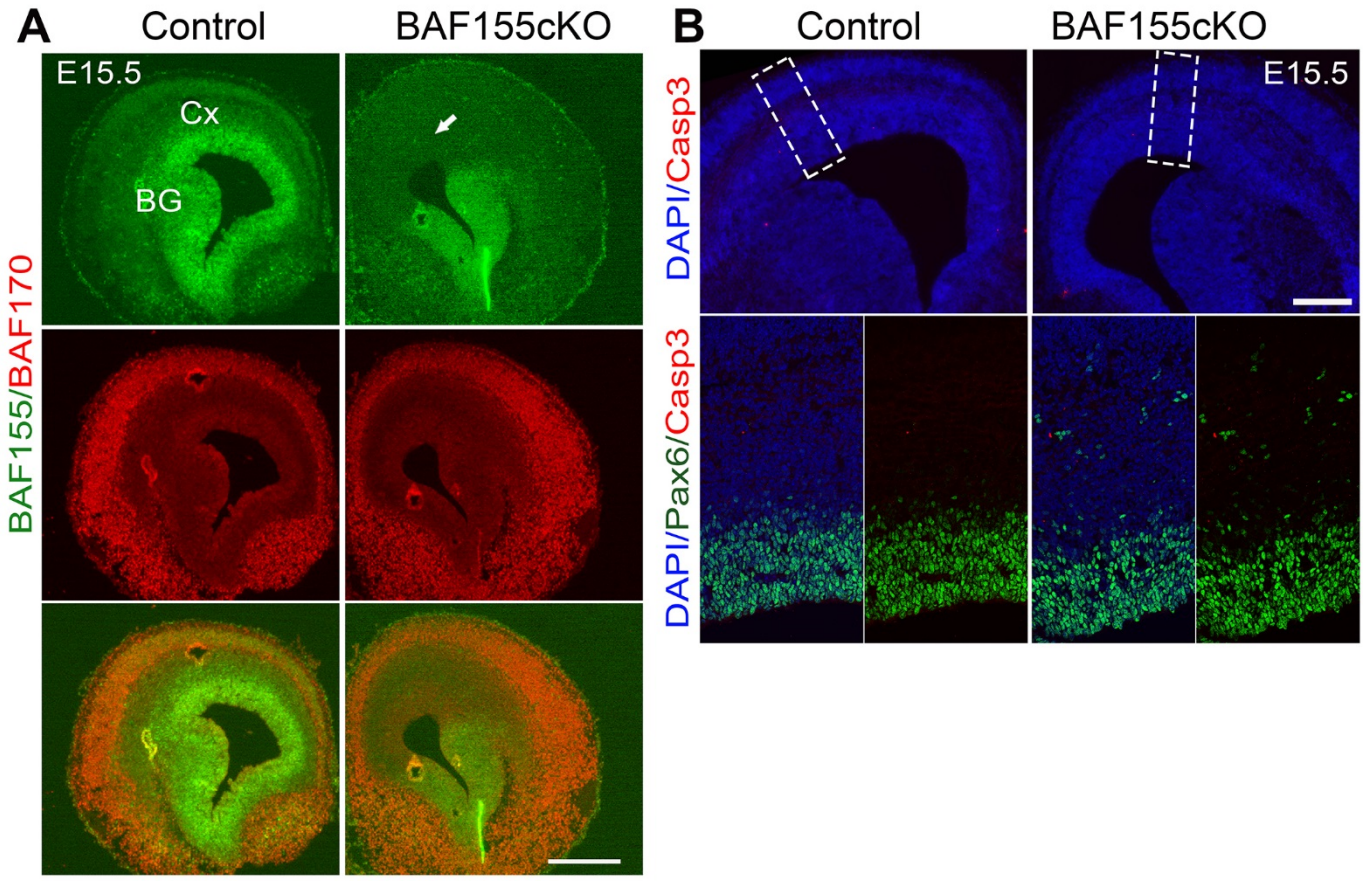

Figure S1 (related to figure 1). Expression of BAF155 and BAF170 in BAF155cKO cortex

(A) IHC using antibodies against BAF155, BAF170 at E15.5 showed a complete loss of BAF155 expression in the pallium (cortex; white arrow) of BAF155cKO compared to control, whereas the expression in the subpallium remains unaltered. However, the expression of BAF170 is unaltered in the BAF155cKO cortex compared to control. (B) IHC using antibodies against cleaved Caspase3 and PAX6 at E15.5 showed no obvious increase in apoptosis both in the entire cortex and specifically in the RG population, labeled by PAX6 immunostaining. Overview images are shown in the upper panel and high magnification confocal image of the lateral cortex (white frame) is shown in the lower panel. [Abbreviations: Cx, cortex; BG, basal ganglia]. Scale bars = 100 μm.

Figure S2

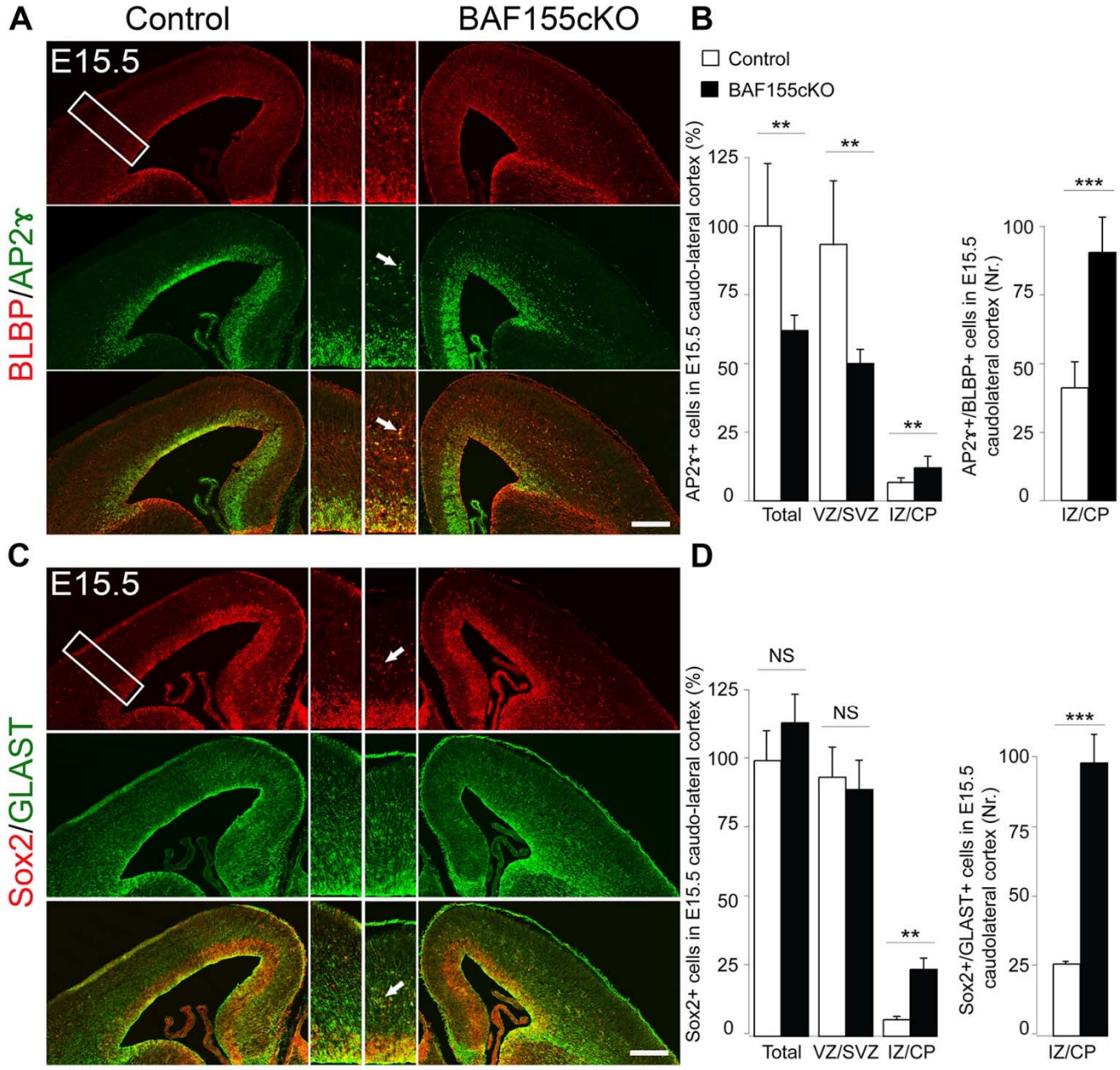
A
Control
BAF155cKO
E15.5
BLBP/AP2γ
B
Control
BAF155cKO
AP2γ+ cells in E15.5 caudo-lateral cortex (%)
125
100
75
50
25
0
**
**
**
Total
VZ/SVZ
IZ/CP
AP2γ+/BLBP+ cells in E15.5 caudolateral cortex (Nr.)
***
IZ/CP
C
E15.5
Sox2/GLAST
D
Sox2+ cells in E15.5 caudo-lateral cortex (%)
NS
NS
**
Total
VZ/SVZ
IZ/CP
Sox2+/GLAST+ cells in E15.5 caudolateral cortex (Nr.)
***
IZ/CP

Figure S2 (related to figure 3, 4). Ectopic basal progenitors in the BAF155cKO cortex express progenitor differentiation markers

(A) IHC using antibodies against BLBP (RG marker) and AP2γ (marker for cells in transition between aRG and bIP fate) in E15.5 control and BAF155cKO cortices. Higher magnifications of the lateral cortex (white frame in overview image) are presented in the middle panels. White arrow indicates BLBP+ AP2γ+ basal progenitors. (B) Statistical analyses showed that in VZ/SVZ, the number of AP2γ+ cells are significantly reduced in the BAF155cKO cortex compared to control. However, there is an increase in AP2γ+ (left graph) and BLBP+ AP2γ+ (right graph) cells in the IZ of mutant cortex. (C) IHC using antibodies against GLAST (cytoplasmic RG marker) and SOX2 (nuclear RG marker) in E15.5 control and BAF155cKO cortices. Higher magnifications of the lateral cortex (white frame in overview image) are presented in the middle panels. White arrow indicates GLAST+ SOX2+ basal progenitors. (D) Statistical analyses showed no significant change in SOX2+ cells in VZ/SVZ of BAF155cKO cortex compared to control. In addition, there is an increase in SOX2+ (left graph) and GLAST+ SOX2+ (right graph) cells in the IZ of mutant cortex. [Abbreviations: VZ, ventricular zone; SVZ, subventricular zone; IZ, intermediate zone; CP, cortical plate]. Values are presented as means ± SEMs (***$p < 0.001$, **$0.001 < p < 0.01$). Scale bars = 100 μm.

Figure S3

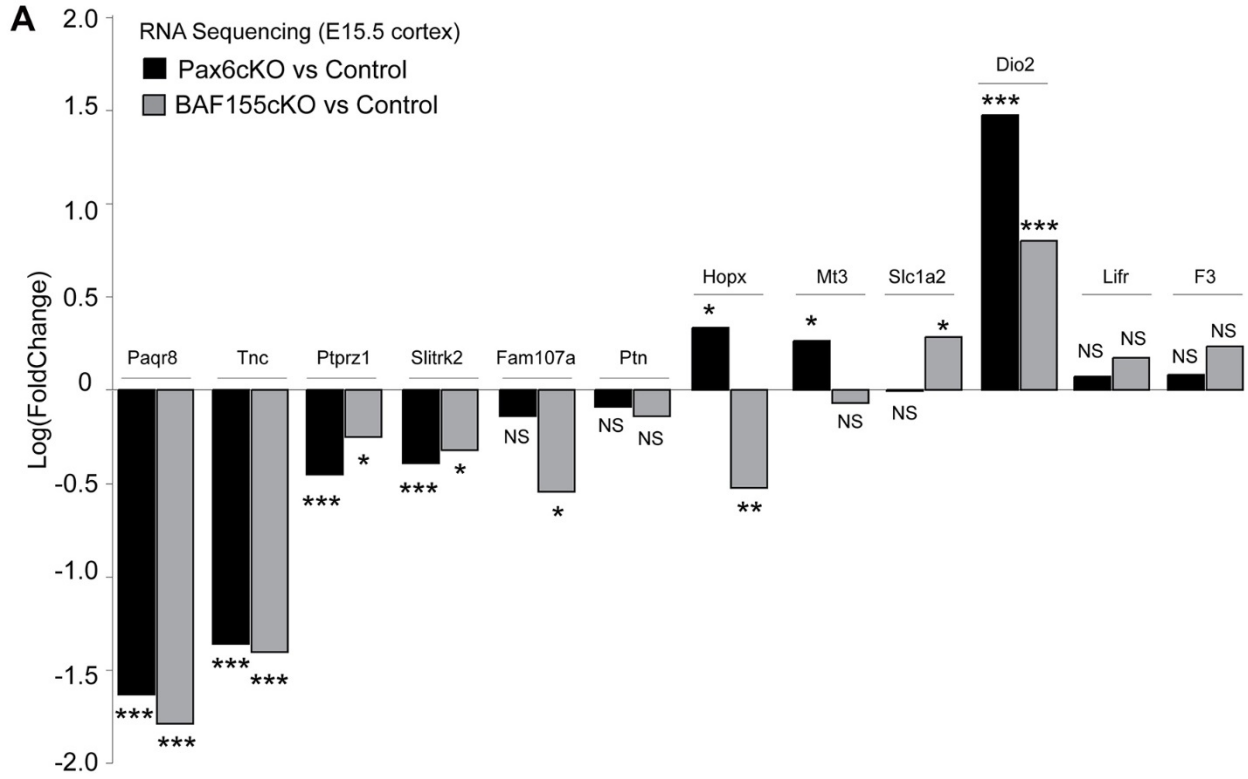
A
RNA Sequencing (E15.5 cortex)
Pax6cKO vs Control
BAF155cKO vs Control
Log(FoldChange)
2.0
1.5
1.0
0.5
0
-0.5
-1.0
-1.5
-2.0
Paqr8
Tnc
Ptprz1
Slitrk2
Fam107a
Ptn
Hopx
Mt3
Slc1a2
Dio2
Lifr
F3
***
NS
*
**

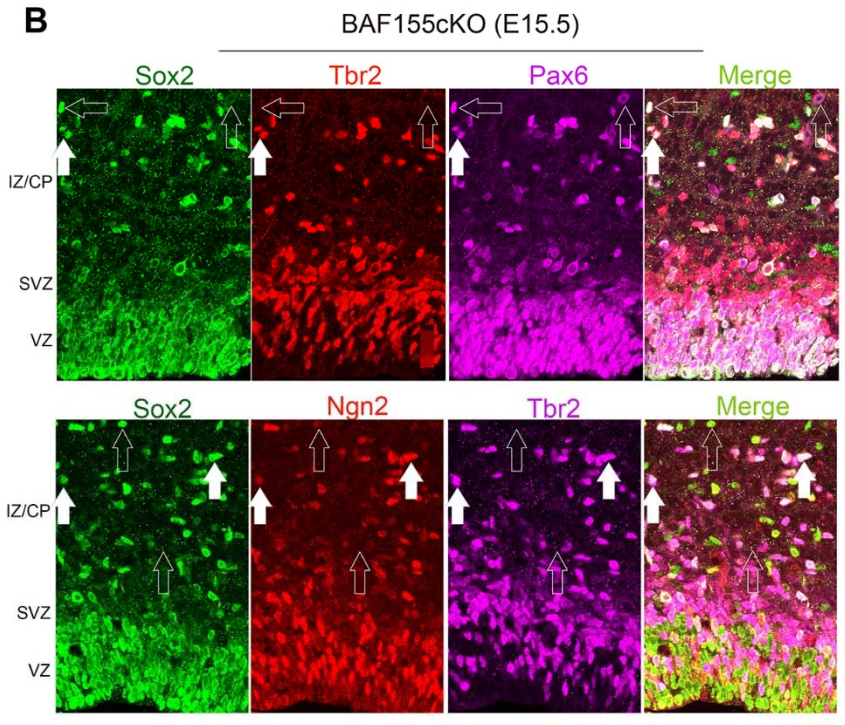
B
BAF155cKO (E15.5)
Sox2
Tbr2
Pax6
Merge
Ngn2
IZ/CP
SVZ
VZ

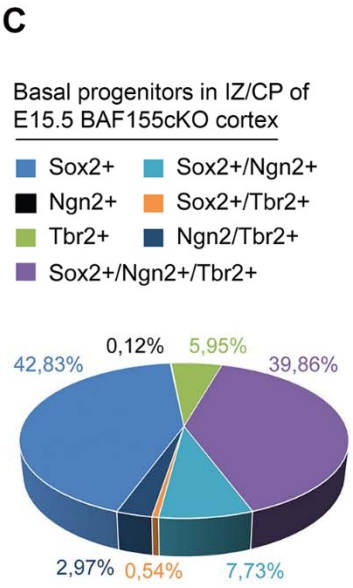
C
Basal progenitors in IZ/CP of E15.5 BAF155cKO cortex
Sox2+
Ngn2+
Tbr2+
Sox2+/Ngn2+/Tbr2+
Sox2+/Ngn2+
Sox2+/Tbr2+
Ngn2/Tbr2+
42,83%
0,12%
5,95%
39,86%
2,97%
0,54%
7,73%

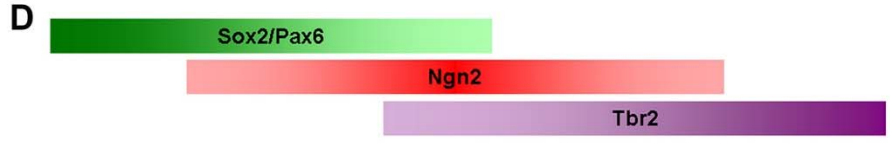
D
Sox2/Pax6
Ngn2
Tbr2

Figure S3 (related to figure 3. 4). Expression of BP molecular markers in BAF155cKO cortex

(A) Expression of bRG-enriched genes in BAF155cKO and PAX6cKO cortex was examined by RNA-seq. (B-D) Cascade-like expression of TFs during generation of excess of ectopic BPs in BAF155cKO mutant. (B) IHC analysis for PAX6, SOX2 (RG markers), NGN2 (marker for cells in transition between RGs and IPs), TBR2 (IP marker) in E15.5 BAF155cKO cortex. (C) Basal progenitors in BAF155-deficit cortex were counted and classified into different categories Based on the expression of SOX2, NGN2, TBR2, the BPs in BAF155cKO IZ/CP belong to different categories: expressing either three markers (SOX2+/NGN2+/TBR2+, 39.86%, filled arrows in B), two markers (SOX2+/NGN2+,7.73%; NGN2+/TBR2+, 2.97% but SOX2+/TBR2+ only in 0.54%, empty arrows in B), or one marker (SOX2, 42.83%; but NGN2 only 0.12%, empty arrows in B). According to present view, a sequential and partially overlapping expression of the TFs PAX6/SOX2→NGN2→TBR2 plays a crucial role for the progressive differentiation of aRGs, giving rise (via bIPs) to glutamatergic neurons of the mouse cortex (Hevner et al., 2006) or bRGs to bIPs toward glutamatergic neurons in human cortex (Hansen et al., 2010). (D) Our findings suggest that activation of such a cascade of TFs is also acting during specification of the ectopic BPs in BAF155 mutant cortex.

Figure S4

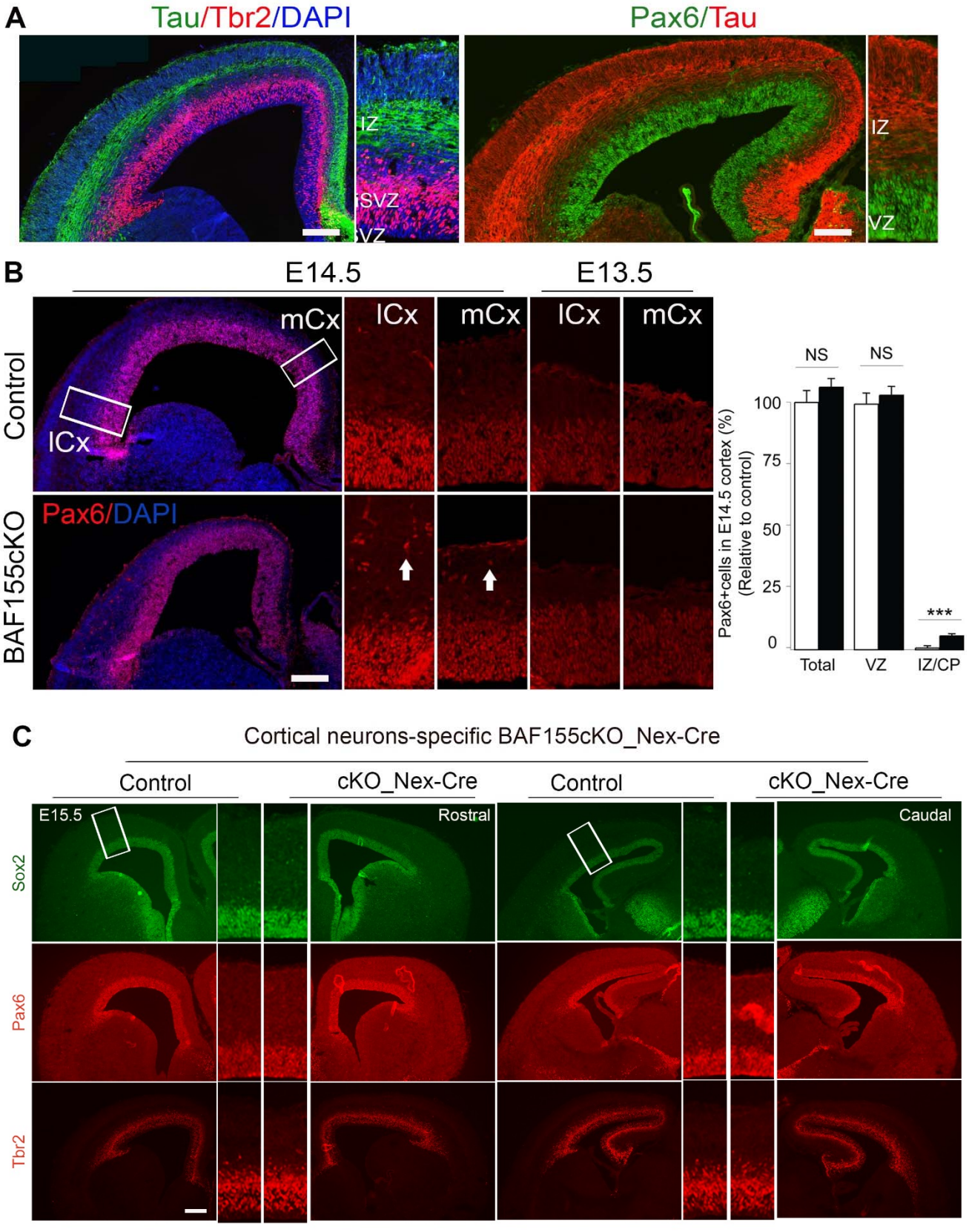
A
Tau/Tbr2/DAPI
IZ
SVZ
VZ
Pax6/Tau
IZ
VZ
B
E14.5
E13.5
Control
BAF155cKO
mCx
lCx
mCx
lCx
mCx
lCx
Pax6/DAPI
NS
NS
Pax6+cells in E14.5 cortex (%)
(Relative to control)
100
75
50
25
0
***
Total
VZ
IZ/CP
C
Cortical neurons-specific BAF155cKO_Nex-Cre
Control
cKO_Nex-Cre
Control
cKO_Nex-Cre
E15.5
Rostral
Caudal
Sox2
Pax6
Tbr2

Figure S4 (related to figure 4). Phenotype of BAF155cKO_*Emx1*-Cre at E13.5-E14.5 and BAF155cKO_*Nex*-Cre at E15.5

(A) IHC using antibodies against TAU/TBR2 (left panel) and TUJ1/PAX6 (right panel) in E15.5 mouse cortex distinguishes VZ/SVZ from the rest of the cortex. The region displaying dense fibers running parallel to apical surface and positive for TAU/TUJ1 markers are identified as IZ. (B) PAX6 IHC with sections of BAF155cKO and control cortices at E13.5 and E14.5 showed ectopic presence of PAX6+ cells in IZ predominantly at E14.5 (white arrows). (D) IHC using antibodies against SOX2, PAX6 (RG markers) and TBR2 (IP marker) in E15.5 control and BAF155cKO_*Nex*-Cre cortices. Higher magnifications of the lateral cortex (white frame in overview image) are presented in the middle panels. Deletion of BAF155 using cortical neuron-specific Cre does not promote generation of basal progenitors in IZ/CP. Values are presented as means ± SEMs (***p <0.001). Scale bars = 100 μm.

Figure S5

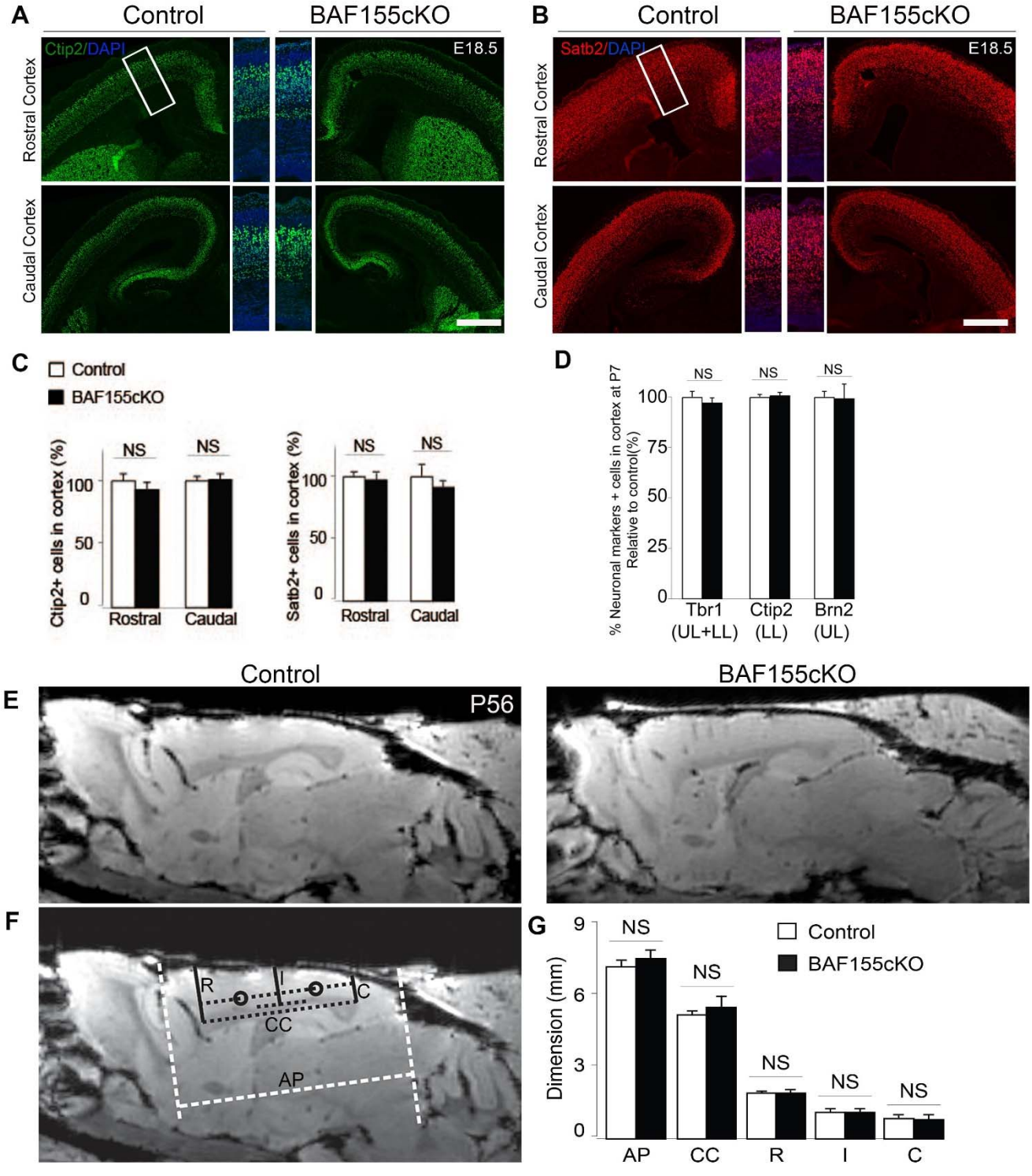
A
Control
BAF155cKO
Ctip2/DAPI
E18.5
Rostral Cortex
Caudal Cortex
B
Control
BAF155cKO
Satb2/DAPI
E18.5
Rostral Cortex
Caudal Cortex
C
Control
BAF155cKO
Ctip2+ cells in cortex (%)
NS
NS
100
50
0
Rostral
Caudal
Satb2+ cells in cortex (%)
NS
NS
100
50
0
Rostral
Caudal
D
% Neuronal markers + cells in cortex at P7
Relative to control(%)
NS
NS
NS
100
75
50
25
0
Tbr1
(UL+LL)
Ctip2
(LL)
Brn2
(UL)
E
Control
BAF155cKO
P56
F
R
I
C
CC
AP
G
Control
BAF155cKO
Dimension (mm)
9
6
3
0
NS
NS
NS
NS
NS
AP
CC
R
I
C

Figure S5 (related to figure 3, 4, 5). BAF155cKO cortex displays normal cortical lamination

(A-C) IHC analysis of CTIP2+ LL (A) and SATB2+ UL (B) neurons in control and BAF155cKO rostral and caudal cortices at E18.5 showed no significant difference in total number (C). (D) Statistical analysis revealed no significant changes in total TBR1+, CTIP2+, BRN2+ neurons between control and BAF155cKO P7 cortices. (E) Representative images of P56 control and BAF155cKO cortices obtained from magnetic resonance imaging (MRI). (F-G) The longest white dashed line is the "AP length". The longest black dashed line is the "CC length". “R”, “I” and “C” denote the distance between CC and pial surface at rostral, intermediate and caudal locations (cortical thickness) respectively (F). None of the above parameters were significantly different comparing control and BAF155cKO cortices (G). Values are presented as means ± SEMs (**0.001<P<0.01, ***P <0.001). [Abbreviations: LL, lower layer; UL, upper layer; AP, anterio-posterior; CC, corpus callosum]. Scale bars = 100 μm.

Figure S6

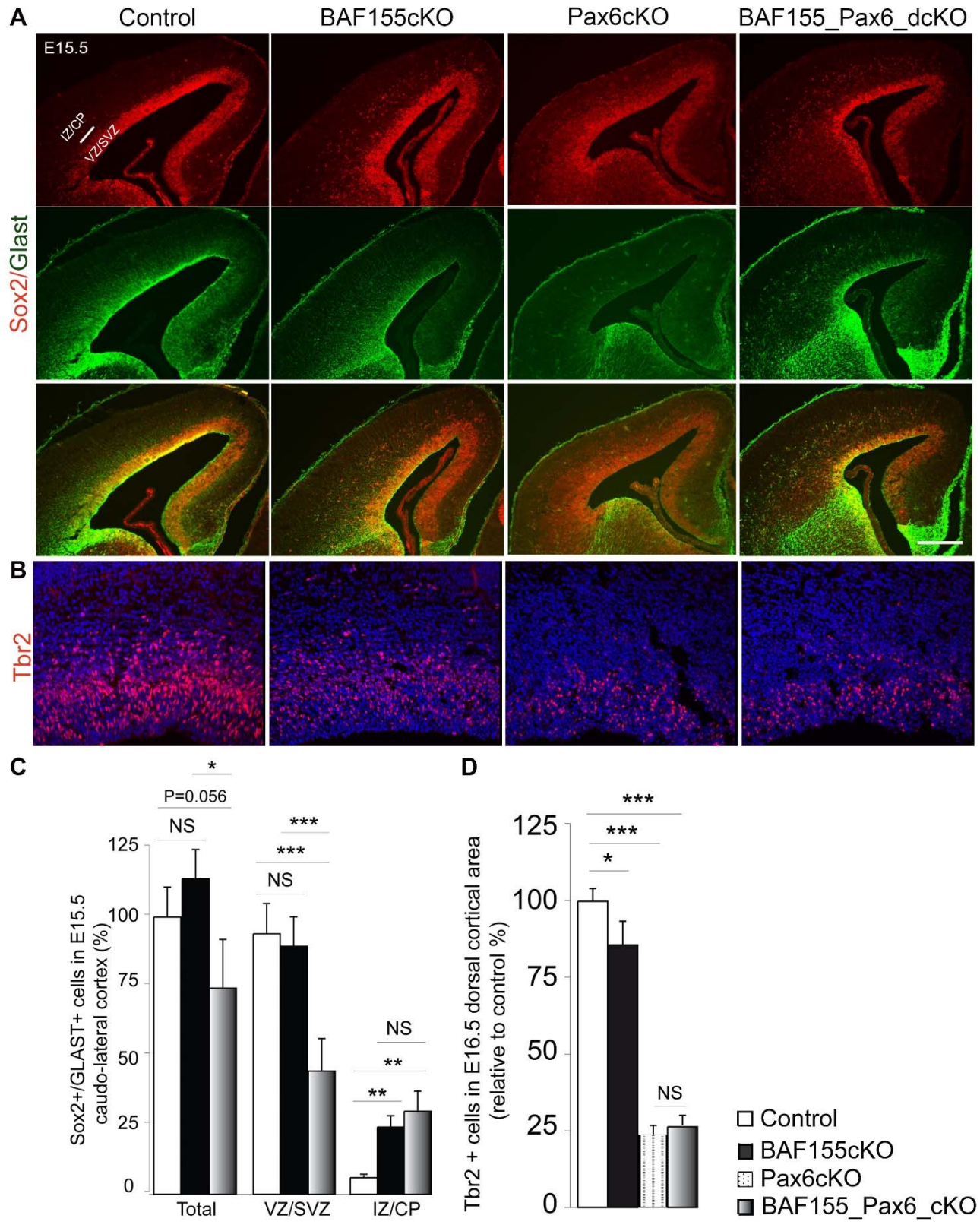
A
Control
BAF155cKO
Pax6cKO
BAF155_Pax6_dcKO
E15.5
IZ/CP
VZ/SVZ
Sox2/Glast
B
Tbr2
C
Sox2+/GLAST+ cells in E15.5 caudo-lateral cortex (%)
125
100
75
50
25
0
*
P=0.056
NS
***
***
NS
NS
**
**
Total
VZ/SVZ
IZ/CP
D
Tbr2 + cells in E16.5 dorsal cortical area (relative to control %)
125
100
75
50
25
0
***
***
*
NS
Control
BAF155cKO
Pax6cKO
BAF155_Pax6_cKO

Figure S6 (related to figure 5). Comparison of bRG and bIPs in BAF155cKO, PAX6cKO and BAF155_PAX6_dcKO mutants

(A, B) IHC using antibodies against nuclear (SOX2), cytoplasmic (GLAST) RG markers (A) and bIPs (TBR2) marker (B) in control, BAF155cKO, PAX6cKO and BAF155_PAX6_dcKO cortices at E15.5 showed bRGs and bIPs in both mutant cortices. (C, D) Statistical analysis revealed that compared to BAF155cKO, loss of PAX6 in addition to BAF155 in dcKO cortex lead to significant reduction in aRGs population in VZ, and a tendency towards increased bRG population in IZ (C). (D) Compared to control, the depleted pool of TBR2+ bIPs was observed in BAF155cKO cortex and more severely in PAX6cKO mutants. Notably, almost equal number of TBR2+ bIPs was seen in PAX6cKO and PAX6_BAF155cKO mutants. Values are presented as means ± SEMs (**0.001<P<0.01, ***P <0.001). Scale bars = 100 μm.

Figure S7

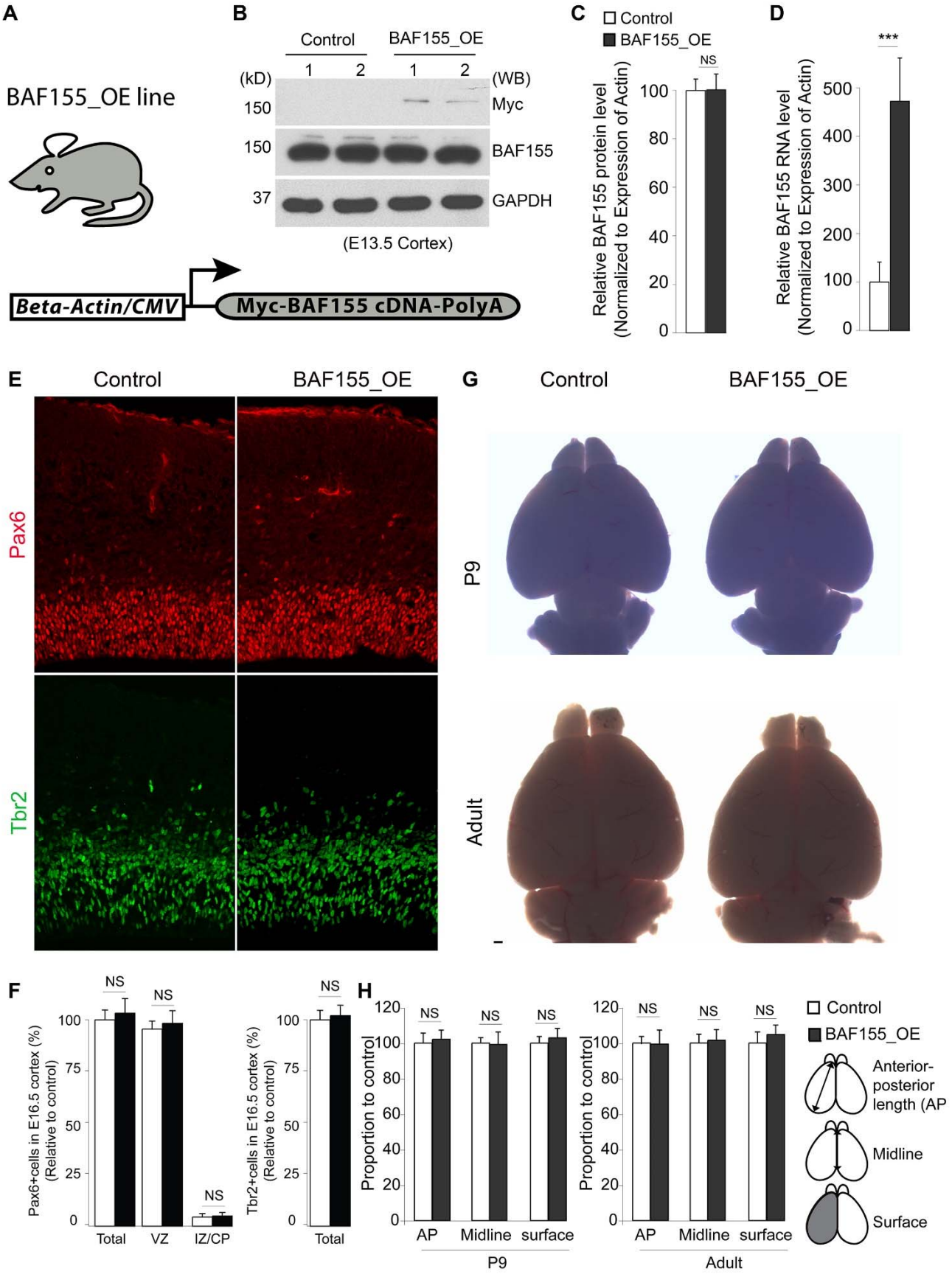
A
BAF155_OE line
Beta-Actin/CMV
Myc-BAF155 cDNA-PolyA
B
Control
BAF155_OE
1 2 1 2
(kD)
(WB)
150
Myc
150
BAF155
37
GAPDH
(E13.5 Cortex)
C
Control
BAF155_OE
NS
Relative BAF155 protein level (Normalized to Expression of Actin)
100
80
60
40
20
0
D
***
Relative BAF155 RNA level (Normalized to Expression of Actin)
500
400
300
200
100
0
E
Control
BAF155_OE
Pax6
Tbr2
G
Control
BAF155_OE
P9
Adult
F
NS
NS
NS
Pax6+cells in E16.5 cortex (%) (Relative to control)
100
75
50
25
0
Total
VZ
IZ/CP
NS
Tbr2+cells in E16.5 cortex (%) (Relative to control)
100
75
50
25
0
Total
H
NS
NS
NS
Proportion to control
120
100
80
60
40
20
0
AP
Midline
surface
P9
NS
NS
NS
Proportion to control
120
100
80
60
40
20
0
AP
Midline
surface
Adult
Control
BAF155_OE
Anterior-posterior length (AP
Midline
Surface

Figure S7 (related to figure 5). Cortical phenotype of transgenic mouse brain upon overexpression of BAF155

(A) Strategy for the generation of transgenic line for BAF155 overexpression (BAF155_OE), described in detail previously (Lee et al., 2007). (B-C) BAF155 Protein (B, C) and RNA (D) levels of tissue samples from BAF155_OE and control cortices at E13.5 were examined by Western blotting and qPCR, respectively. Relative levels of BAF155 protein (C) and RNA (D) are presented in the diagrams. As compared to control, a highly-increased level of BAF155 mRNA in BAF155_OE cortex was observed (D). Notably, BAF155_OE cortex has only mild enhanced level of exogenous BAF155 protein (BAF155-myc, B), but not total BAF155 protein (B, C). (E, F) IHC (E) and quantitative (F) analyses showed no difference in the number of for PAX6+RGs and TBR2+bIPs in the cortex of BAF155 mutants compared with controls at E16.5 (G, H) morphological (G) and statistical analysis indicated that there is no difference in anterior-posterior (AP), midline length, and cortical surface of BAF155_OE and control cortices at P9 and adult stages. Values are presented as means ± SEMs (*P < 0.05; **P < 0.01; ***P <0.005; n = 4, cortical tissues from 4 control and 4 OE embryos).

Figure S8

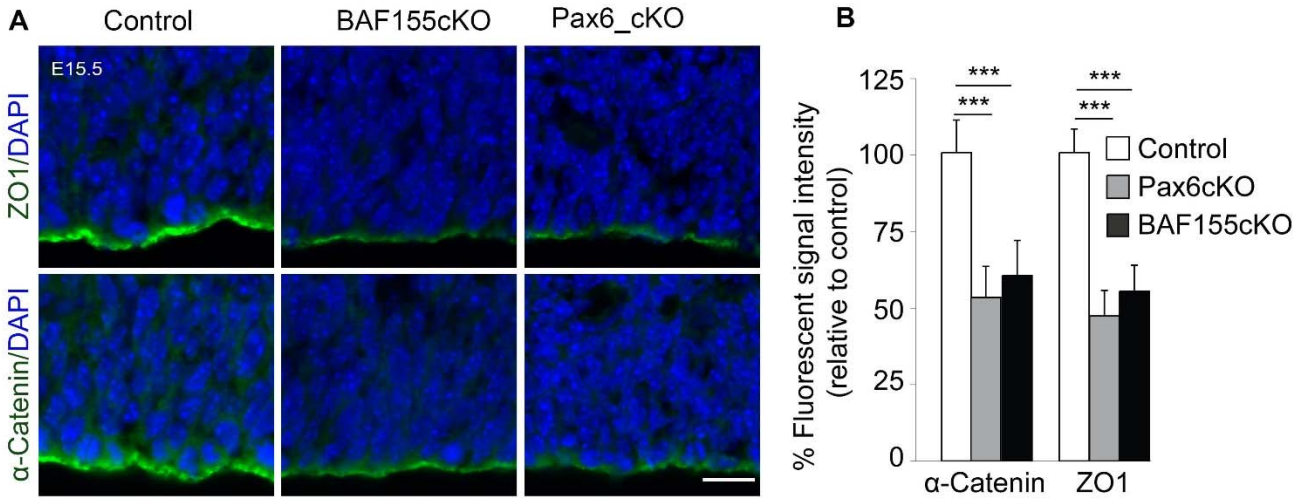
A
Control
BAF155cKO
Pax6_cKO
E15.5
ZO1/DAPI
α-Catenin/DAPI
B
% Fluorescent signal intensity
(relative to control)
125
100
75
50
25
0
***
***
***
***
Control
Pax6cKO
BAF155cKO
α-Catenin
ZO1

Figure S8 (related to figure 6). Expression of adherens junction molecules in BAF155- and PAX6- deficient cortex

(A, B) immunostaining of coronal sections from the control, BAF155cKO and PAX6cKO cortex at E15.5 for ZO1 and α-Catenin (A) and quantitative analysis revealed a loss of expression of these adherens junction marker in apical surface of mutants. Values are presented as means ± SEMs (*P < 0.05; **P < 0.01; ***P <0.005; n = 6). Scale bars = 50 μm.

Figure S9

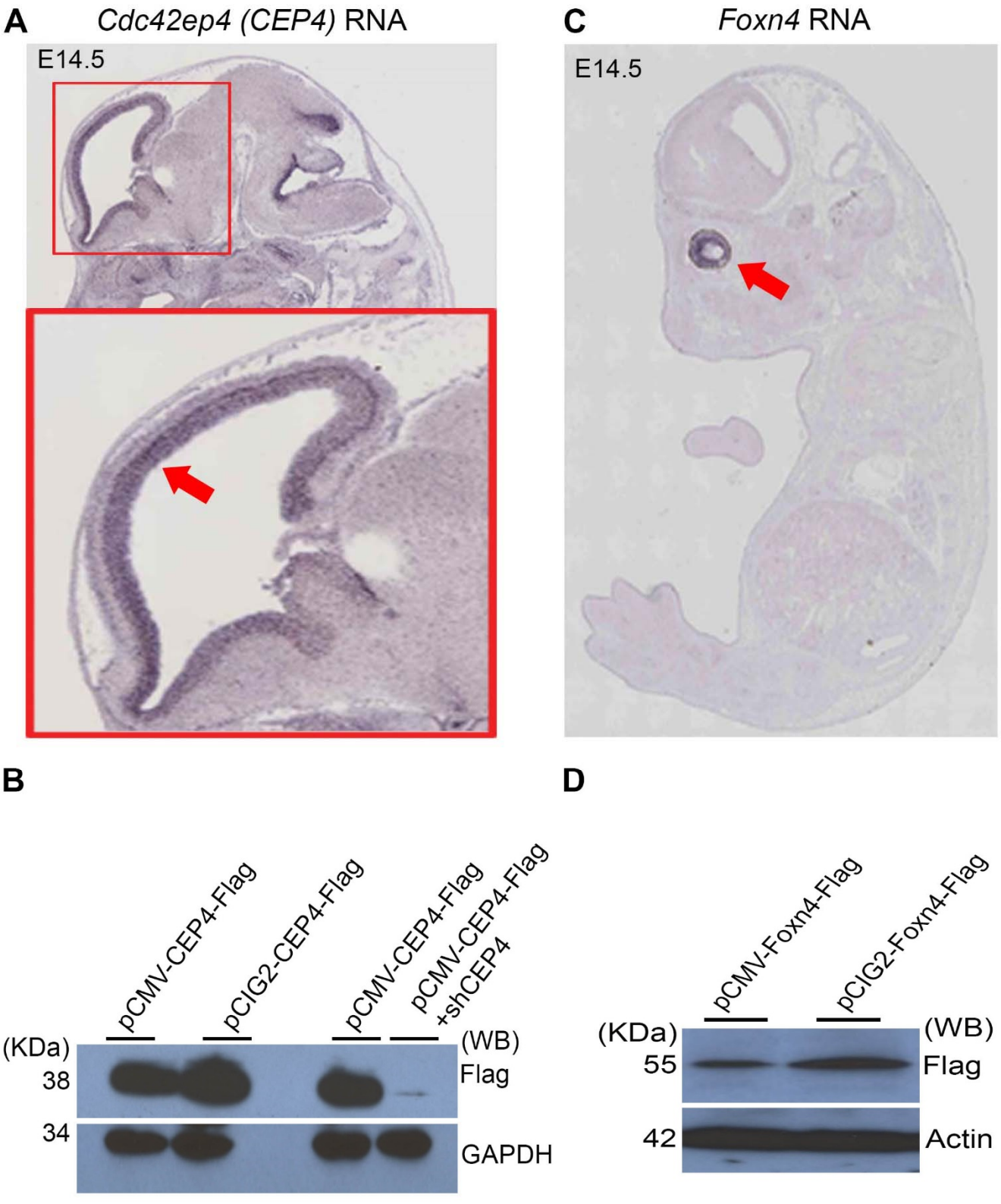
A
Cdc42ep4 (CEP4) RNA
E14.5
C
Foxn4 RNA
E14.5
B
pCMV-CEP4-Flag
pCIG2-CEP4-Flag
pCMV-CEP4-Flag
pCMV-CEP4-Flag +shCEP4
(KDa)
38
34
(WB)
Flag
GAPDH
D
pCMV-Foxn4-Flag
pCIG2-Foxn4-Flag
(KDa)
55
42
(WB)
Flag
Actin

Figure S9 (related to figure 6, 7). *Cep4* and *Foxn4* as candidate genes downstream of BAF155 in developing cortex

(A) *In situ* hybridization for *Cep4* in sagittal section of E14.5 mouse embryo obtained from GenePaint database (Visel et al., 2004). Higher magnification of the cortex shows a specific localization of *Cep4* transcripts in the pallial ventricular zone (arrows). (B) HEK293T cells were transiently transfected with the respective flag-tagged plasmid(s) as indicated and cell lysates collected after 48 hours were tested by western blotting (GAPDH used as a loading control). The expression levels of the CMV- and pCIG2-CEP4 plasmids (the first two lanes) and the efficiency of short hairpin (sh) construct against CEP4 (last two lanes) were tested. The shCEP4 and pCIG2-CEP4 was subsequently used for IUE experiments. (C) *In situ* hybridization for *Foxn4* in sagittal section of E14.5 mouse embryo from GenePaint database shows retina-specific localization of *Foxn4* transcripts and absence in cortex. (D) HEK293T cells were transiently transfected with the respective flag-tagged plasmid(s) and cell lysates collected after 48 hours were tested by western blotting (Actin used as a loading control). First and second lane shows the expression levels of the CMV- and pCIG2-FOXN4 plasmids respectively. pCIG2-FOXN4 was subsequently used for IUE experiment.

TRANSPARENT METHODS

Plasmids

Plasmids used in this study: pCON-P3-Luc (2xP6CON plus 3xP3 sequences in pGL3 basic, Promega as described in Tuoc & Stoykova, 2008); pCIG2-ires-eGFP, pCIG2-Cre-ires-eGFP (gift from Dr. Francois Guillemot, NIMR London, Hand et al., 2005); pLuc-Ssx2ip, pLuc-Wnt5a, pLuc-Fgfr1, pLuc-Celsr1, pLuc-Pdgfrb, pLuc-Cdc42ep1 and pLuc-Cdc42ep4 (PCR based amplification of respective gene promoter from genomic DNA followed by cloning into pGL3 basic, Promega); shCEP4 (custom made); pLuc-Cux1 (Tuoc et al., 2013a); pLuc-Ngn2 (Scardigli et al., 2003) as a gift from Dr. Francois Guillemot, NIMR London; pLuc-Tbr2 (Ochiai et al., 2009) as a gift from Dr. Miyata, Nagoya University; pCIG2-CEP4 (CEP4 ORF cDNA cloned into pCIG2-ires-eGFP); pCIG2-BAF170, pCIG2-BAF155 (Tuoc et al., 2013a; Tuoc et al., 2013b);

Antibodies

The following polyclonal (pAb) and monoclonal (mAb) primary antibodies used in this study were obtained from the indicated commercial sources: Actin-beta (1:500, Sigma), AP2γ mouse mAb (1:100; Abcam), BAF155 mouse mAb (1:100; Santa Cruz), BAF170 rabbit pAb (Bethyl), BLBP rabbit pAb (1:200; Chemic), Brn2 goat pAb (1:100; Santa Cruz), Casp-3 rabbit pAb (1:100; Cell Signaling), Ctip2 rat pAb (1:200; Abcam), Flag mAb (1:1000; Sigma), GAPDH rabbit pAb (Santa Cruz), GFP (1:400, Abcam), GLAST pAb pig (1:500; Frontier), Luciferase (1:2000, Abcam), Ngn2 (1:20, Santa Cruz), Pax6 mAb mouse (1:100; Developmental Studies Hybridoma Bank), phospho-H3 rat pAb (1:300; Abcam), pVim mouse mAb (1:500; MBL), Sox2 mouse mAb (1:100; R&D Systems), Tau (1:200, Millipore), Tbr1 rabbit pAb (1:300; Chemicon), Tbr2 rabbit pAb (1:200; Abcam), Tuj mouse mAb (1:500; Chemicon).

Secondary antibodies used were peroxidase-conjugated goat anti-rabbit IgG (1:10000; Covance); peroxidase-conjugated goat anti-mouse IgG (1:5000; Covance); peroxidase-conjugated goat anti-rat IgG (1:10000; Covance); and Alexa 488-, Alexa 568-, Alexa 633- and Alexa 647-conjugated IgG (various species, 1:400; Molecular Probes).

Transgenic mice and *in utero* electroporation

Floxed *Baf155* (Choi et al., 2012), floxed *Pax6 (Ashery-Padan et al., 2000)*, *Emx1-Cre* (Gorski et al., 2002), and *Nex-Cre* (Goebbels et al., 2006) mice were maintained in a C57BL6/J background. Animals were handled in accordance with the German Animal Protection Law, with the permission of the Bezirksregierung Braunschweig and University Medical Centre Goettingen animal experimentation committee. *In utero* electroporation was performed as described previously (Tuoc et al., 2013a; Tuoc and Stoykova, 2008).

Luciferase assay

Putative PAX6 binding sites in the promoter regions of the candidate genes (*Ssx2ip, Wnt5a, Fgfr1, Celsr1, Pdgfrb, Cdc42ep1, Cdc42ep4*) were identified from published data (Xie et al., 2013), the respective regions were amplified from mouse genomic DNA and inserted into the pGL3 vector (Promega). These firefly luciferase-based reporter gene constructs were transfected along with a renilla expression vector into Neuro2A cells in a 24-well plate using Lipofectamine 2000 (Life Technologies). The cells were cultured for 48 h after which cell extracts were prepared and assayed for luciferase activity with the use of a Dual-Luciferase Reporter Assay System (Promega) following manufacturer's protocol, such that the firefly luciferase-based reporter gene activity was normalized to the renilla control in all cases.

WB, Immunohistochemistry

WB and IHC experiments were carried out as previously described (Narayanan et al.; Tuoc et al., 2009).

Spindle Angle Analysis

Cortical sections were stained with pVIM, a cytoplasmic marker to identify RG cell shape and process and pHH3, a nuclear marker to identify dividing cells at anaphase and early telophase. Images of z-stack sections were taken by SP5 confocal microscopy and 3D reconstruction of the confocal stacks was done as described previously (Postiglione et al., 2011; Tuoc et al., 2013a).

DiI labeling

Mouse brains were dissected out in cold PBS and fixed in cold 4% PFA in PBS at 4°C overnight, followed by removal of the meninges that covers the cortical surface. The DiI crystals (Life Technologies) were dissolved in 100% ethanol to a final concentration of 1 mg/ml in 1 ml final volume. Then each brain sample was transferred to 1 ml fresh 4% PFA in PBS added with 30 ml of 1 mg/ml DiI solution and incubated at 37°C for another 24 hr. After DiI labeling, brains were washed with

PBS, sectioned on the vibratome (Leica VT1200S) into 100 mm slices, and stained with PAX6 antibody and DAPI before mounting.

Magnetic Resonance Imaging (MRI)

MRI was performed *ex vivo* on the brain of five wild-type and four BAF155cKO mice at the age of 8 weeks at 9.4 T (Bruker Biospin MRI GmbH, Ettlingen, Germany). Radiofrequency excitation and signal reception were accomplished with the use of a birdcage resonator (inner diameter 72 mm) and a 4-channel phased-array surface coil, respectively (both Bruker Biospin MRI GmbH, Ettlingen, Germany). Three-dimensional proton-density-weighted MRI was performed with a 3D gradient-echo sequence (radiofrequency-spoiled FLASH, repetition time = 22 ms, echo time = 7.6 ms, flip angle = 15°, fat suppression = 90°, measuring time = 66 min.) at an isotropic resolution of 100 µm. For evaluation of signal intensities, anatomically defined cross-sections were obtained from the original 3D MRI data sets by multiplanar reconstructions using software supplied by the manufacturer (Paravision 5.0, Bruker Biospin MRI GmbH, Ettlingen, Germany). The plane crossing the anterior as well as posterior commissure served as a reference for the selection of standardized sections to facilitate comparisons with minimized intra- and interindividual variability. The analysis followed a strategy previously developed for intra- and inter-individual comparisons of MR images (Watanabe et al., 2015).

RNA-Sequencing

RNA was extracted (RNAeasy kit, Qiagen) from pallium of 4 control, 4 PAX6cKO, 4 BAF155cKO E15.5 littermate embryos. cDNA libraries were prepared with the TruSeq RNA Sample Preparation v2 Kit. The amount was measured in Nanodrop and the quality in Agilent 2100 Bioanalyzer. Base calling, fastq conversion, quality control, read alignment were all performed as outlined for ChIP-Seq. Reads were aligned to mouse genome mm10 and counted with FeaturesCount (http://bioinf.wehi.edu.au/featureCounts/). Differential expression was assessed using DESeq2 from Bioconductor (Love et al., 2014). Functional GO enrichment analysis was performed with ToppGene (Chen et al., 2009).

RNA-seq analysis

The presented p-values are non-adjusted. We preferred to use non-adjusted p-values in order to minimize the likelihood of missing out interesting genes, which could have been culled out with a stricter cut-off. This approach enables us to see the bigger picture and general trends with more clarity, especially when performing the overlaps or GO category analyses. We have however looked into the RNA-Seq data with much stricter cut-offs – adjusted p-value < 0.05 & |fold change| > 1.5, and the conclusions confirm the same trend. There are 443 genes down- and 316 genes upregulated in BAF155cKO mice compared to controls. And there are 866 genes down- and 820 genes upregulated in PAX6cKO mice compared to controls. The RNA-Seq data has been deposited in GEO under accession number GEO:GSE106711 and will be released to public upon acceptance of the manuscript.

qRT-PCR

Total RNA isolated from E15.5 cortices (Control: n=6, PAX6cKO: n=6, BAF155cKO: n=6). The purified RNA was quantified spectrophotometrically and used in quantitative RT-PCR analyses employing the QuantiTect Rev.Transcription and the QuantiTect SYBR Green PCR Kits (Qiagen). The assays were performed with n= 6 and normalized to internal 18S. Statistical comparisons were carried out using Student's t-test. The results are presented as means ± SEM. qPCR primers were purchased from Qiagen.

Quantification of cell number

IHC quantification was performed using anatomically matched coronal or sagittal sections as mentioned in the experiments. For each antigen that was stained and quantitatively studied, cell counts in at least four matched sections were averaged from three biological replicates (control/experiment pairs). For quantitative measurements of cells positive: e.g. TBR2/NGN2 (Fig. 3), SOX2/PAX6 (Fig. 5), PAX6/TBR2 (Fig. 6, 7), AP2γ /BLBP (Fig. S2) and SOX2/GLAST (Fig. S2, S5) labeled cells were counted within a 200 µm strip of dorso-lateral cortex. For cells positive for CTIP2/SATB2 (Fig. S4 A-C), labeled cells were counted within a 100 µm strip of dorso-lateral pallium in anatomically matched sections of rostral and caudal cortex.

For cells positive for PAX6 (Fig. 4, E15.5), labeled cells were counted in the pallium in anatomically matched sections of rostral, medial and caudal cortex and represented as total positive cells. For cells positive for PAX6 (Fig. 4, E16.5), labeled cells were counted in the pallium in anatomically matched sections of medial cortex. For cells positive for PAX6 (Fig. S3), labeled cells were counted in the indicated white frames and represented as total positive cells.

For cells positive for TBR1/CTIP2/BRN2 (Fig. S4 D), labeled cells were counted within a 100 µm strip each at the rostral, medial and caudal regions of anatomically matched sagittal sections; the combined cell count was represented as total positive cells. All cell counts were normalized to control group and represented as percentage (%).

Relative quantification of cortical size

Parameters of cortical size were measured and analysed as described by O'Leary et al (Bishop et al., 2003; Bishop et al., 2002; Sahara and O'Leary, 2009; Tuoc et al., 2013). Shortly, forebrains of mutants and controls at P9 and adult with their presented dorsal view were photographed under a dissection microscope. Cortical arterial/posterior axis (A/P), cortical surface and midline lengths from the digitized images were processed to compare above parameters between mutants and controls by using NIH ImageJ software.

Imaging, quantification, and statistical analyses

Images were captured using Axio Imager M2 (Zeiss) with a Neurolucida system, and confocal fluorescence microscopy (TCS SP5; Leica). Images were further processed with Adobe Photoshop. IHC signal intensities were quantified by using ImageJ software, as described previously (Narayanan et al.; Tuoc and Stoykova, 2008).

Statistical comparisons were carried out using Student's *t*-test. The results are presented as means ± SEM. All details of statistical analyses for histological experiments are presented in Table S6.

SUPPLEMENTAL REFERENCES

Ashery-Padan, R., Marquardt, T., Zhou, X., and Gruss, P. (2000). Pax6 activity in the lens primordium is required for lens formation and for correct placement of a single retina in the eye. Genes Dev *14*, 2701-2711.

Chen, J., Bardes, E.E., Aronow, B.J., and Jegga, A.G. (2009). ToppGene Suite for gene list enrichment analysis and candidate gene prioritization. Nucleic acids research *37*, W305-311.

Choi, J., Ko, M., Jeon, S., Jeon, Y., Park, K., Lee, C., Lee, H., and Seong, R.H. (2012). The SWI/SNF-like BAF complex is essential for early B cell development. J Immunol *188*, 3791-3803.

Goebbels, S., Bormuth, I., Bode, U., Hermanson, O., Schwab, M.H., and Nave, K.A. (2006). Genetic targeting of principal neurons in neocortex and hippocampus of NEX-Cre mice. Genesis *44*, 611-621.

Gorski, J.A., Talley, T., Qiu, M., Puelles, L., Rubenstein, J.L., and Jones, K.R. (2002). Cortical excitatory neurons and glia, but not GABAergic neurons, are produced in the Emx1-expressing lineage. J Neurosci *22*, 6309-6314.

Hansen, D.V., Lui, J.H., Parker, P.R., and Kriegstein, A.R. (2010). Neurogenic radial glia in the outer subventricular zone of human neocortex. Nature *464*, 554-561.

Hevner, R.F., Hodge, R.D., Daza, R.A., and Englund, C. (2006). Transcription factors in glutamatergic neurogenesis: conserved programs in neocortex, cerebellum, and adult hippocampus. Neurosci Res *55*, 223-233.

Lee, Y.S., Sohn, D.H., Han, D., Lee, H.W., Seong, R.H., and Kim, J.B. (2007). Chromatin remodeling complex interacts with ADD1/SREBP1c to mediate insulin-dependent regulation of gene expression. Molecular and cellular biology *27*, 438-452.

Love, M.I., Huber, W., and Anders, S. (2014). Moderated estimation of fold change and dispersion for RNA-seq data with DESeq2. Genome biology *15*, 1.

Narayanan, R., Pham, L., Kerimoglu, C., Watanabe, T., Kiszka, K.A., Rosenbusch, J., Seong, R.H., Fischer, A., Stoykova, A., Staiger, J.F*., et al.* Chromatin remodeling BAF155 subunit regulates the genesis of basal progenitors in developing cortex

Ochiai, W., Nakatani, S., Takahara, T., Kainuma, M., Masaoka, M., Minobe, S., Namihira, M., Nakashima, K., Sakakibara, A., Ogawa, M*., et al.* (2009). Periventricular notch activation and asymmetric Ngn2 and Tbr2 expression in pair-generated neocortical daughter cells. Mol Cell Neurosci *40*, 225-233.

Postiglione, M.P., Juschke, C., Xie, Y., Haas, G.A., Charalambous, C., and Knoblich, J.A. (2011). Mouse inscuteable induces apical-Basal spindle orientation to facilitate intermediate progenitor generation in the developing neocortex. Neuron *72*, 269-284.

Scardigli, R., Baumer, N., Gruss, P., Guillemot, F., and Le Roux, I. (2003). Direct and concentration-dependent regulation of the proneural gene Neurogenin2 by Pax6. Development *130*, 3269-3281.

Tuoc, T.C., Boretius, S., Sansom, S.N., Pitulescu, M.E., Frahm, J., Livesey, F.J., and Stoykova, A. (2013a). Chromatin Regulation by BAF170 Controls Cerebral Cortical Size and Thickness. Developmental Cell *25*, 256-269.

Tuoc, T.C., Narayanan, R., and Stoykova, A. (2013b). BAF chromatin remodeling complex: cortical size regulation and beyond. Cell Cycle *12*, 2953-2959.

Tuoc, T.C., Radyushkin, K., Tonchev, A.B., Pinon, M.C., Ashery-Padan, R., Molnar, Z., Davidoff, M.S., and Stoykova, A. (2009). Selective cortical layering abnormalities and behavioral deficits in cortex-

specific Pax6 knock-out mice. The Journal of neuroscience : the official journal of the Society for Neuroscience *29*, 8335-8349.
Tuoc, T.C., and Stoykova, A. (2008). Trim11 modulates the function of neurogenic transcription factor Pax6 through ubiquitin-proteosome system. Genes & development *22*, 1972-1986.
Visel, A., Thaller, C., and Eichele, G. (2004). GenePaint.org: an atlas of gene expression patterns in the mouse embryo. Nucleic Acids Res *32*, D552-556.
Watanabe, T., Frahm, J., and Michaelis, T. (2015). Reduced intracellular mobility underlies manganese relaxivity in mouse brain in vivo: MRI at 2.35 and 9.4 T. Brain structure & function *220*, 1529-1538.
Xie, Q., Yang, Y., Huang, J., Ninkovic, J., Walcher, T., Wolf, L., Vitenzon, A., Zheng, D., Gotz, M., Beebe, D.C*., et al.* (2013). Pax6 interactions with chromatin and identification of its novel direct target genes in lens and forebrain. PLoS One *8*, e54507.